Search for supersymmetry with R-parity violation at $\sqrt{s}$ = 192 to 202 GeV

R. Barbier, N. Benekos, C. Berat, P. Jonsson, F. Ledroit-Guillon, R. Lopez-Fernandez, E. Merle, T. Papadopoulou, V. Poireau

DELPHI Collaboration

DELPHI 2000-084 CONF 383
11 July, 2000

Search for supersymmetry with R–parity violation at $\sqrt{s} = 192$ to 202 GeV

R. Barbier[1], N. Benekos[2], C. Berat[3], P. Jonsson[1], F. Ledroit-Guillon[3], R. López-Fernández[3], E. Merle[3], Th. Papadopoulou[2], V. Poireau[4]

[1]IPN Lyon, [2]N.T.U. Athens, [3]ISN Grenoble, [4]CEA/DAPNIA/SPP Saclay.

Abstract

Searches for pair and single production of supersymmetric particles under the assumption of non-conservation of R–parity with a dominant $LL\bar{E}$ or $\bar{U}\bar{D}\bar{D}$ term have been performed using the data collected by the DELPHI experiment at LEP in e^+e^- collisions at centre-of-mass energies of 192, 196, 200 and 202 GeV. No excess of data above Standard Model expectations was observed. The results were used to constrain the MSSM parameter space and to derive mass limits on supersymmetric particles.

Contributed Paper for ICHEP2000

1 Introduction

In 1999, the LEP centre-of-mass energy reached 192-196-200-202 GeV, and an integrated luminosity of about 226 pb^{-1} has been collected by the DELPHI experiment. The data have been analyzed to search for supersymmetric particles in the hypothesis of R–parity violation ($\not{R}_p$) [1]. The major consequences of the non conservation of the R–parity is the allowed decay of the Lightest Supersymmetric Particle (LSP) in standard fermions and the possibility to produce single supersymmetric particles. The analyses of this note cover both single and pair productions of supersymmetric particles. The $\not{R}_p$ superpotential [2] contains three trilinear terms, two violating L conservation, and one violating B conservation. We consider here only the $\lambda_{ijk}\mathrm{L}_i\mathrm{L}_j\bar{\mathrm{E}}_k$ (non conservation of L) and $\lambda''_{ijk}\bar{\mathrm{U}}_i\bar{\mathrm{D}}_j\bar{\mathrm{D}}_k$ (non conservation of B) terms (i, j, k are generation indices), which couple the sleptons to the leptons and the squarks to the quarks respectively.

The Minimal Supersymmetric Standard Model (MSSM) scheme [3] with the assumption that the gaugino masses are unified at the Grand Unified Theories (GUTs) scale is assumed. Relevant parameters for these $\not{R}_p$ searches are then: M_1, M_2, the U(1) and SU(2) gaugino mass at the electroweak scale (with $\mathrm{M}_1 = \frac{5}{3}tan^2\theta_W\mathrm{M}_2$), m_0, the scalar common mass at the GUT scale, μ, the mixing mass term of the Higgs doublets at the electroweak scale and tanβ, the ratio of the vacuum expectation values of the two Higgs doublets. We assume that the running of the λ and λ'' couplings from the GUT scale to the electroweak does not have a significant effect on the "running" of the gaugino and fermion masses.

The LSP is assumed to have a negligible lifetime so that the production and decay vertices coincide. Otherwise the LSP decay vertex is displaced, and the analyses described here become inefficient.

1.1 *R*–parity violating decays of supersymmetric particles

1.1.1 Direct and Indirect decays

Two types of supersymmetric particle decays are considered. First, the direct decay of a sfermion into two standard fermions, or the decay of a neutralino (chargino) into a fermion and a virtual sfermion which then decays into two standard fermions. Second, the indirect decay corresponding to the supersymmetric particle cascade decay through R–parity conserving vertex to on-shell supersymmetric particles down to the lighter supersymmetric particle which then decays via one $\mathrm{LL\bar{E}}$ or $\mathrm{\bar{U}\bar{D}\bar{D}}$ term.

1.1.2 Decays through $\mathrm{LL\bar{E}}$ terms

The direct decay of a neutralino or a chargino via a dominant λ_{ijk} coupling leads to purely leptonic decay signatures, with or without neutrinos ($ll'\nu$, $ll'l''$, $l\nu\nu$). The indirect decay of a heavier neutralino or a chargino adds jets and/or leptons to the leptons produced in the LSP decay.

The sneutrino direct decay gives two charged leptons: via λ_{ijk} only the $\tilde{\nu}_i$ and $\tilde{\nu}_j$ are allowed to decay directly to $l_j^{\pm}l_k^{\mp}$ and $l_i^{\pm}l_k^{\mp}$ respectively. The charged slepton direct decay gives one neutrino and one charged lepton (the lepton flavor may be different from the slepton one). The supersymmetric partner of the right-handed lepton, $\tilde{l}_{kR}$ can only decay directly to in $\nu_{iL}l_{jL}$ or $l_{iL}\nu_{jL}$.

The indirect decay of a sneutrino (resp. charged slepton) into a neutralino and a neutrino (resp. charged lepton) leads to a purely leptonic final state: two charged leptons and two neutrinos (resp. three charged leptons and a neutrino). With a $LL\bar{E}$ term, only the indirect decay of a squark into a quark and a neutralino (or a chargino) is possible.

When the charged leptons are τ (for example with λ_{131} or λ_{133} couplings), additional neutrinos are generated in the τ decay, producing more missing energy in the decay and leading to a smaller number of charged leptons in the final state.

1.1.3 Decays through $\bar{U}\bar{D}\bar{D}$ terms

In case of a dominant $\bar{U}\bar{D}\bar{D}$ term, the neutralino decays via a virtual squark and a quark and subsequently gives a three quarks final state (the squark decays into two quarks via $\bar{U}\bar{D}\bar{D}$ terms). Then for each indirect decay of a chargino, squark or slepton pair we have at least six quarks in the final state. Therefore the most important feature of these decays are the number of quarks produced which goes up to ten for the indirect decay of two charginos with the hadronic decays of the W bosons. The direct stop and sbottom decays gives the smallest number of quarks in the final state and were not considered in the squark analysis. In this channel, a large amount of hadronic decay of WW and ZZ bosons remain as an irreducible background for the four-jet signal. The unique possibility for the sleptons to decay through a $\bar{U}\bar{D}\bar{D}$ term is the indirect decay channel. In this last case, two leptons are produced in the slepton decay in association with the six jets coming from the two neutralinos. A 6 jets + 2 leptons final state is the signature of these signals.

1.2 Pair production of supersymmetric particles

Pair production of supersymmetric particles in MSSM with $\not{R}_p$ is exactly identical to the pair production with R_p conservation, since the trilinear couplings are not present in the production vertex.

The mass spectrum of neutralinos and charginos is determined by the three parameters of the MSSM theory assuming GUT scale unification of gaugino masses: M_2, μ and $\tan\beta$. The charginos are produced by pairs in the s-channel via γ or Z exchange, or in the t-channel via sneutrino ($\tilde{\nu}_e$) exchange if the charginos have a gaugino component; the neutralinos are produced by pairs via s-channel Z exchange provided they have a higgsino component, or via t-channel selectron exchange if they have gaugino a component. The t-channel contribution is suppressed when the slepton masses (depending on m_0) are high enough. When the selectron mass is sufficiently small (less than 100 GeV/c^2), the neutralino production can be enhanced, because of the t-channel $\tilde{e}$ exchange contribution. On the contrary, if the $\tilde{\nu}_e$ mass is in the same range, the chargino cross-section can decrease due to destructive interference between the s- and t-channel amplitudes.

Pair production cross-section of sfermions mainly depends on the sfermion masses. The selectron and sneutrino cross-sections are also very sensitive to the neutralino and chargino components (function of μ, M_2 and $\tan\beta$) via the t-channel exchange. In the case of the third generation, the left-right mixing angle enters in the production cross-section as well. Two cases were considered in the stop and sbottom analyses to extract mass limits: the first one with no mixing, the second one with the mixing angle corresponding to the squarks decoupling from the Z boson.

1.3 Single sparticle production

At LEP, resonant[1] sneutrino production is allowed via the coupling λ_{121} or λ_{131}. The cross-section for a sneutrino (J=0) can be expressed as [4]:

$$\sigma(e^+e^- \to \tilde{\nu} \to X)(s) = \frac{4\pi s}{M^2_{\tilde{\nu}}} \frac{\Gamma(ee)\Gamma(X)}{(s - M^2_{\tilde{\nu}})^2 + M^2_{\tilde{\nu}}\Gamma^2_{\tilde{\nu}}}$$

where $\Gamma(ee) = \Gamma(\tilde{\nu}_j \to e^+e^-) = \frac{\lambda^2_{1j1}}{16\pi} M_{\tilde{\nu}_j}$, $j = 2, 3$, and $\Gamma(X)$ denotes the partial width for $\tilde{\nu}$ decay to final state X, with $X = e^+e^-$ (direct decay), $X = \tilde{\chi}^0\nu$ or $X = \tilde{\chi}^{\pm}l^{\mp}$ (indirect decays of the sneutrino).

Given the present upper limits on λ_{121} and λ_{131} derived from indirect searches of R–parity violating effects [5, 6], the e^+e^- decay channel ($\sigma \propto \lambda^4$) is suppressed compared to the other two ($\sigma \propto \lambda^2$), unless both the neutralino and the chargino are heavier than the sneutrino. The direct decay mode is investigated by the LEP collaborations by looking for deviations to the Standard Model in the cross-sections and asymmetries of $e^+e^- \to l^+l^-$. The indirect decay channels are analyzed explicitly here, taking into account any mass and the actual width of the $\tilde{\nu}$ as a function of the MSSM parameters.

2 Data samples

The data recorded in 1999 by the DELPHI experiment at centre-of-mass energies from $\sqrt{s} = 192$ GeV to 202 GeV (Table 2), corresponding to a total integrated luminosity of 226.1 pb^{-1}, have been analysed. The DELPHI detector has been described elsewhere [7].

To evaluate background contaminations, different contributions coming from the Standard Model processes were considered. The Standard Model events were produced by the following generators:

- $\gamma\gamma$ events: `BDK` [8] for $\gamma\gamma \to l^+l^-$ processes, and `TWOGAM` [9] for $\gamma\gamma \to$ hadron processes.
- two-fermion processes: `BHWIDE` [10] for Bhabhas, `KORALZ` [11] for $e^+e^- \to \mu^+\mu^-(\gamma)$ and for $e^+e^- \to \tau^+\tau^-(\gamma)$ and `PYTHIA` [12] for $e^+e^- \to q\bar{q}(\gamma)$ events.
- four-fermion processes: `EXCALIBUR` [13] and `GRC4F` [14] for all types of four fermion processes: non resonant ($f\bar{f}f'\bar{f}'$), simply resonant ($Zf\bar{f}$, $Wf\bar{f}'$) and doubly resonant (ZZ, WW) (`PYTHIA` was used also for cross checks).

Signal events were generated with the `SUSYGEN` program [15] followed by the full DELPHI simulation and reconstruction program (`DELSIM` [7]). A faster simulation (`SGV` [16]) was used in the analyses performed when a $LL\bar{E}$ term is dominant was used to check that the efficiencies were stable at points without full simulation compared to their values at the nearest points determined with the full simulation.

[1] We disregard here the t-channel contributions present for second and third generation final leptons for reasons of compactness. These contributions are included in the signal simulation and final estimation of expected events.

3 Description of the analyses

For all the analyses presented in this section, it was assumed that only one λ_{ijk} or λ''_{ijk} is dominant at a time, and its upper bound, derived from indirect searches of R–parity violating effects [4]–[6], has been taken into account for the generation of the signals.

3.1 Search for pair production in case of $\mathrm{LL\bar{E}}$ terms

Two types of analyses have been performed:

- the first one assumes that λ_{122} is dominant (i.e the charged leptons coming from $\not{R}_p$ decay are muons and electrons). This is the most efficient and selective case since the selection criteria are based on e and μ identification;
- the second search assumes that λ_{133} is dominant, meaning that the leptons from $\not{R}_p$ decay are mainly taus and electrons. This is the case with the lowest efficiency and the lowest rejection power due to the presence of several taus in the final state.

Any of the possible topologies should be covered by one of the two analysis types, to be sure that any type of $\not{R}_p$ via $\mathrm{LL\bar{E}}$ terms signal could be discovered. Two different λ_{ijk} can lead to the same final state, and therefore the same efficiency ranges. This allows to apply the first type of analysis to signals produced via λ_{232}. In most cases, the analyses of the second type are applied to signals generated with other λ_{ijk}, and the efficiencies are either of the same order or higher than for λ_{133} signals.

The applied selections were based on the criteria already presented in [17, 18], using mainly missing momentum and energy, lepton identification and kinematic properties, and jet characteristics. The lepton identification is based on standard DELPHI algorithms.

- The electron identification is provided by the `REMCLU` [19] package; different levels of tagging which classify the electrons with respect to the criteria they verify can be obtained: a "loose" tag is obtained from less severe criteria than a "tight" tag. In the analyses described in this section a particle is a well identified electron if it verifies the tight conditions from `REMCLU`, if its momentum is greater than 8 GeV/c and if there is no other charged particle in a 2^o cone around it.
- The muon identification algorithm relies on the association of charged particles with signals from the muon chambers, providing with four levels of tag, the two most severe levels are "standard" and "tight". In the analyses described in this section a particle is a well identified muon if its momentum is greater than 5 GeV/c and if it is tagged as a standard or tight muon candidate by the DELPHI algorithm [7].

As already mentioned, indirect decays of gaugino pairs can give two or more jets in the final state, beside leptons and missing energy. Moreover, in the case of the λ_{133} coupling, thin jets can be produced in the τ decays. The jets were reconstructed with the `DURHAM` [20] algorithm. In order to cover the different topologies, the jet number was not fixed, and the number of charged particles in the jet could be low (thin jets with one charged particle for instance). In the following, the transition value of the y_{cut} in the `DURHAM` algorithm at which the event changes from a n-jet to a $(n{-}1{=}m)$-jet configuration is noted y_{nm} or y_n.

3.1.1 $LL\bar{E}$ term: charginos and neutralinos searches

The $\widetilde{\chi}_i^0$ and $\widetilde{\chi}_k^\pm$ pair productions were considered for different values of tanβ (from 1 to 30), m_0 (between 90 GeV/c^2 and 500 GeV/c^2), μ (between –200 GeV/c^2 and 200 GeV/c^2) and M_2 (between 5 and 400 GeV/c^2), for both λ_{122} and λ_{133} searches.

Common preselection

In the search for neutralino and chargino pair production in case of a dominant λ_{122} or λ_{133} coupling, the preselection requirements described in [18] were used. A criterion has been added, completing the preselection stage: the thrust axis has been asked not to be parallel to the beam pipe, i.e. $|\cos\theta_{\rm th}|$ less than 0.9. The preselection was efficient to suppress 99.9% of the backgrounds coming from Bhabha scattering and two-photon processes while removing 97% of the $f\bar{f}\gamma$ contribution. The preselection also reduced by 75% the four-fermion contamination.

Since no signal has been observed, only the results of the λ_{133} analysis are used to derive the most conservative limits, and then the λ_{122} analysis is not detailed in the present note.

Analyses with λ_{122} as dominant coupling

Concerning the neutralino and chargino searches with a dominant λ_{122} coupling, the selection procedure has been adapted from the sequential analysis performed at 189 GeV [18]; it is detailed in [21]. At the end of the selection, no event remained in the data, compared to 1.7 ± 0.1 expected from Standard Model processes contributing to the background (0.6 from W^+W^- events and the rest from other four-fermion processes).

Using the events produced with `DELSIM`, selection efficiencies have been studied on $\widetilde{\chi}_1^0\widetilde{\chi}_1^0$ and $\widetilde{\chi}_1^+\widetilde{\chi}_1^-$ signals. All gaugino pair production processes which contribute significantly have been simulated altogether for each MSSM studied point, using `SUSYGEN`. A global event selection efficiency has then been determined at each point.
The selection efficiencies were in the range 30–50% for the neutralino pair production and 40–65% for the chargino pair production.

Analyses with λ_{133} as dominant coupling

The analysis applied to 1999 data was an update of the analysis used for 1998 data. The selection criteria were studied to be efficient for both low and high multiplicity cases. First, a refined preselection was done after the common preselection: lower limit on missing energy was applied, i.e. $E_{\rm miss}$ greater than $0.3\times\sqrt{s}$ and the acollinearity had to be greater than 7° for events with more than 6 charged particles.

For events with a charged particle multiplicity from four to six, corresponding to neutralino direct decays, the following criteria were applied:

- the energy of the most energetic lepton had to be between 2 and 70 GeV;
- there should be no other charged particle in a 20° (6°) half cone around any identified lepton for a charged particle multiplicity equal to 4 (5 or 6);
- the number of neutral particles had to be less than 11.

For events with a charged particle multiplicity greater than six, the previous criteria

became:

- the energy of the most energetic lepton had to be between 5 and 60 GeV;
- if there was only one identified lepton, there should be no other charged particle in a 6° half cone around it, if there were more than one identified lepton there should be no other charged particle in a 10° half cone around at least two of them;
- the number of neutral particles had to be less than 15;
- at least one electron (loose identification) was required.

In all cases, the polar angle of at least one lepton had to be between 40° and 140°. These criteria removed 95% of $f\bar{f}\gamma$, ZZ and W^+W^- events.

The selection based on the jet characteristics and topologies was then applied. First, constraints have been imposed to y_{nm} values; this criterion eliminated 99% of the remaining $f\bar{f}\gamma$ contribution. In events with more than six charged particles, at least one jet with low charged particle multiplicity was demanded. In four- or five-jet configurations, a minimum number of charged jets was required. In case of a four-jet topology, a cut was applied on the value of $E^j_{\rm min} \times \theta^{j_a j_b}_{\rm min}$ where $E^j_{\rm min}$ is the energy of the less energetic jet, and $\theta^{j_a j_b}_{\rm min}$ is the angle between the two closest jets. These requirements reduced the background from 4-fermion processes.

The number of remaining real data and simulated background events after the selection are reported in Table 3. A good agreement between the number of observed and expected background events was obtained, and no excess was observed in data: 14 candidates remained in the data, compared to 15.6 ± 0.8 expected from Standard Model background processes (13.7 from W^+W^- events and the rest from other four-fermion processes).

The selection efficiencies were computed from simulated samples for different points of the MSSM parameters space. A global event selection efficiency has been determined at each point. It was in the range 12–37% for the neutralino pair production and 21-33% for the chargino pair production.

3.1.2 LL$\bar{\rm E}$ term: sleptons searches

In case of sneutrino direct decay ($\mathrm{Br}(\tilde{\nu} \rightarrow \ \ell^+\ell^-) = 100\%$), the processes $\tilde{\nu}_{\rm e}\bar{\tilde{\nu}}_{\rm e} \rightarrow 4\mu$ (λ_{122}), $\tilde{\nu}_{\rm e}\bar{\tilde{\nu}}_{\rm e} \rightarrow 4\tau$ (λ_{133}), $\tilde{\nu}_{\mu}\bar{\tilde{\nu}}_{\mu} \rightarrow 4\tau$ (λ_{233}) and $\tilde{\nu}_{\tau}\bar{\tilde{\nu}}_{\tau} \rightarrow 2e2\tau$ (λ_{133}) have been generated for different values of sneutrino mass up to 98 GeV/c^2, with tanβ and μ fixed at 1.5 and –150 GeV/c^2 respectively. In order to be sure that all final states were covered, signals obtained for other λ_{ijk} couplings and for sneutrino mass around 85 GeV/c^2 were also generated. Events with sneutrino (slepton) indirect decay ($\mathrm{Br}(\tilde{\nu}\ (\tilde{l}) \ \rightarrow \tilde{\chi}^0_1\nu\ (\ell)) = 100\%$) were also simulated with λ_{122} and λ_{133} couplings, for different $\tilde{\nu}$ ($\tilde{l}$) and $\tilde{\chi}^0_1$ masses, in order to cover several ranges of mass difference between sneutrinos (sleptons) and neutralinos. Furthermore, in case of slepton indirect decays, selectron, smuon and stau pair productions have been simulated, since the efficiencies depend also on the slepton flavor.

Contrary to the gaugino search, in the slepton search it was not possible to define a common preselection for λ_{122} and λ_{133} analyses.

Analyses when λ_{122} coupling is dominant

These analyses were designed to cover three main topologies:

- 4μ and 2μ2e (no missing energy), from the direct decay of $\widetilde{\nu}_{\rm e}$ and $\widetilde{\nu}_{\mu}$ pair, respectively;
- 4 leptons and missing energy, with at least 2 muons, from the indirect decay of any sneutrino pair;
- 6 leptons and missing energy, with at least 4 muons, from the indirect decay of $\widetilde{\mu_R}^+\widetilde{\mu_R}^-$.

Events with a number of charged particles greater than or equal to four and greater than the number of neutral particles were selected. At least one identified lepton and another charged particle should both be in the barrel (i.e. with a polar angle between 40° and 140°). When neutrinos are produced in the decays, as in indirect decays, a minimum value of 5 GeV/c for the missing transverse momentum $\not{p}_t$ was required, and the polar angle of the missing momentum should be between 27° and 153°. But these could not be applied to the 4μ or 2e2μ final states. In this particular case, a minimum value of 2 GeV/c was required for $\not{p}_t$, and to compensate the loss in selectivity, a lower limit to the total energy from the charged particles was applied and at least one identified muon was demanded, which eliminated Bhabha scattering events at the preselection stage. Requiring the thrust axis to be not parallel to the beam pipe, i.e. $|\cos\theta_{\rm th}|$ less than 0.9, completed the preselection stage, and after it, a vast majority of the Bhabha scattering (all in case of 4μ channel) and $\gamma\gamma$ events were eliminated.

After the preselection, the main background sources were the $\rm f\bar{f}(\gamma)$ and the four-fermion events. Lower or upper cut on missing energy was applied, depending on the type of final state. An additional criteria on the maximal energy of the most energetic photon was used to remove events with such energetic photon in the selection of the 4μ final states. Several criteria concerning the identified leptons were applied: the number of well identified muons, the isolation angle between each identified lepton and the closest charged particle, and eventually the energy of the most energetic lepton. All these criteria helped to reduce the remaining $\rm f\bar{f}(\gamma)$ and four-fermion events.

No excess of candidate events was found in the 1999 data.

Analyses when λ_{133} coupling is dominant

With this type of coupling, mainly taus are produced in the final states. Then there are always neutrinos coming from the τ decay, eventually with additional neutrinos which could be produced at the $\not{R}_p$ vertex.

The analyses were designed to cover two main topologies:

- the 2τ2e final states (missing energy coming from the tau decay only), from the direct decay of $\widetilde{\nu}_{\tau}$ pairs;
- the 4 or 6 leptons and missing energy final states, with at least 2 taus, from the indirect decay of any sneutrino pair; and from the indirect decay of a slepton pair.

A same preselection procedure can be settled for the two analyses.

Preselection
In the preselection step, it was required:

- the number of charged particles greater than three, and at least two of them with a polar angle between 40° and 140°;
- at least one "tightly" identified lepton;
- the total energy greater than $0.10\times\sqrt{s}$
- the missing p_t greater than 5 GeV/c;
- the thrust axis to be not parallel to the beam axis ($|\cos\theta_{\rm th}| < 0.9$);
- the polar angle of the missing momentum between 27° and 153°;
- the acollinearity had to be greater than 2° and greater than 7° if there were more than six charged particles.

This was efficient to suppress the background coming from Bhabha scattering and two-photon processes, and to remove a large part of the $f\bar{f}(\gamma)$ contribution. After this preselection stage, 1262 events were selected for 1209 ± 5 expected from the background sources. The distribution of the energy from the charged particles obtained before the requirement on the acollinearity, and the distribution of the missing energy at the preselection stage are shown in Figure 1.

Channels with high amount of missing energy
One analysis was performed in order to study three different cases:

- the channel $\widetilde{\nu}_{\rm e}\bar{\widetilde{\nu}}_{\rm e} \rightarrow 4\tau$ (direct decay of $\widetilde{\nu}_{\rm e}$);
- the channel $\tilde{\nu}\bar{\tilde{\nu}}\rightarrow \nu\widetilde{\chi}^0_1\nu\widetilde{\chi}^0_1$ (indirect decay of sneutrinos);
- the channel $\tilde{\ell}^+_R\tilde{\ell}^-_R \rightarrow \ell\widetilde{\chi}^0_1\ell\widetilde{\chi}^0_1$ (indirect decay of scalar leptons).

In all cases, the final state has a large amount of missing energy, and mainly taus. The criteria were very similar to those described in [18]; they are listed in Table 4. The distributions of the number of neutral particles, and of the largest lepton isolation angle obtained after the requirement on the missing energy are shown in Figures 2–a, 2–b; the distributions of the number of leptons in the barrel and of the Durham variable y_{32}, obtained after the requirement on the lepton isolation are shown in Figures 2–c, 2–d. All these variables were used in the selection. At the end of the selection, 3 events remained in the data compared to 3.9 ± 0.3 expected from the Standard Model processes. The background was mainly composed of four-fermion events, in particular from the W pair production.

In case of direct decay of $\widetilde{\nu}_{\rm e}$, the analysis efficiency was between 27% and 36%, depending on the sneutrino mass. It laid in the same range for the sneutrino indirect decay, depending also on the neutralino mass, but not on the sneutrino flavour. The efficiencies were higher for final states obtained in indirect decay of slepton pairs, due to the presence of two additional leptons. They ranged from 31% to 45% for stau pairs, and were 5% to 8% higher for selectron and smuon pairs (in this case indeed the two additional leptons are either electrons or muons).

Channel with low $E_{\rm miss}$ ($ee\tau\tau$)
Compared to the previous selection procedure, the major change was the suppression of the criterion on the missing energy, and the introduction of the requirement to have at least one well identified electron. Beside this, some other criteria were slightly modified, such as the number of charged particles (from 4 to 7), the energy of the most energetic lepton (between 25 and 80 GeV). After these requirements, 15 events were obtained compared

to 12.8 ± 0.7 from the Standard Model processes. Then, criteria on jet properties were applied (see Table 5). The agreement between data and Standard Model background expectation is fairly good (see Figure 3). At the end of the selection, 4 candidates were obtained for 4.5 ± 0.8 expected. The efficiencies varied with the $\tilde{\nu}_\tau$ mass and ranged from 45% to 51%.

3.1.3 LL$\bar{\text{E}}$ term: stop searches

In the case of stop pair production, each of the stops decays into a charm quark and a neutralino, and, with the subsequent $\not{R}_p$ decay of the neutralino into leptons, the final state is composed of two jets + four charged leptons + missing energy. Signals corresponding to these stop pair decays were generated for several sets of stop and neutralino masses.

The analysis performed in the case of a dominant λ_{133} coupling is detailed, since it leads to the most conservative limit on the stop mass.

The same preselection criteria as described in Section 3.1.2 were used, but since in the case of stop pair production the final state always contains two jets, a minimum multiplicity of eight charged particles was required. No requirement was applied on the thrust axis, on the other hand, a stonger criteria was applied on the polar angle of the missing momentum ($30^\circ \leq \theta_{\text{miss}} \leq 150^\circ$) The preselection was efficient to suppress the background coming from Bhabha scattering and two-photon processes, and to remove a large part of the $\text{f}\bar{\text{f}}(\gamma)$ contribution. After this preselection stage, 1274 events were selected for 1231 ± 5 expected from the background sources.

The criteria used to select the final states of the stop pair indirect decay are listed in Table 6. The missing energy had to be at least $0.3\sqrt{s}$, and the charged and neutral particle multiplicity were limited to 25 and 20 respectively. Then, requirements based on the lepton characteristics were applied:

- the polar angle of at least one lepton had to be between 40° and 140°;
- the energy of the most energetic identified lepton had to be greater between 5 and 50 GeV;
- an isolation criterion was imposed (at least one lepton with no other charged particle in a 6° half cone around it);
- at least one well identified electron.

The selection based on the jet characteristics and topologies was then applied. First, constraints have been imposed to y_{nm} values. In four-jet configuration, at least one jet with low charged particle multiplicity was required. 19 events remained after the selection procedure, with 20.0 ± 0.5 expected from background contribution (see Table 6). The main background contribution comes from the W^+W^- production.

The selection efficiencies varied with the stop mass and with the mass difference between the stop and the lightest neutralino. They laid around 30%, except in two cases: for low neutralino masses, the efficiencies were around 18–20%, and in the degenerate case (i.e the mass lower than 5 GeV/c^2), the efficiency decreased and went down to almost 0 for $m_{\tilde{t}} - m_{\tilde{\chi}^0} = 2$ GeV/c^2. This analysis was not optimized for topologies produced when the mass difference is below 5 GeV/c^2, therefore it was not sensitive to the very degenerate case.

3.2 Search for pair production in case of $\bar{\mathrm{U}}\bar{\mathrm{D}}\bar{\mathrm{D}}$ terms

The present studies covered the search for $\widetilde{\chi}_1^0$, $\widetilde{\chi}_1^+$, $\widetilde{q}$ and $\widetilde{l}$ pair production previously studied with the data collected by DELPHI in 1997 and 1998 [22]. The analysis of the different decay channels can be organized on the basis of the number of hadronic jets in the final state (see Table 1).

Clustering algorithm
For each multi-jet analysis, the clustering of hadronic jets was performed by the *ckern* package [23] based on the Cambridge clustering algorithm [24]. For each event, *ckern* provides all possible configurations between 2 and 10 jets. The values of the variables y_{nm} (for n between 2 and 10), was a powerful tool to identify the topologies of the multi-jet signals.

Signal selection with neural networks
A neural network method was applied in order to distinguish signals from Standard Model background events for all multi-jet analyses except for the 6 jets + 2 muons analysis which have been performed with a sequential method (the very good muon identification of the detector gave sufficient signal discrimination from hadronic background). The SNNS package [25] and MLPFit package [26] were used for the training and the validation of the neural networks. The training was done on samples of simulated background and signal. The exact configuration and input variables of each neural network depended on the search channel. Each neural network provided a discriminant variable which was used to select the final number of candidate events for each analysis.

3.2.1 $\bar{\mathrm{U}}\bar{\mathrm{D}}\bar{\mathrm{D}}$ term: chargino and neutralino searches

The following preselection criteria were applied:

- the number of charged particles had to be greater than 15,
- the total energy was required to be greater than $0.6 \times \sqrt{s}$,
- the energy of charged particles was required to be greater than $0.3 \times \sqrt{s}$,
- the effective centre-of-mass energy had to be greater than 150 GeV,
- the discriminating variable $\mathrm{d}_\alpha = \alpha_{min} \times E_{min} - 0.5 \times \beta_{min} \times E_{max}/E_{min}$ had to be greater than -10 rad.GeV; in the d_α definition, α_{min} is the minimum angle between two jets, β_{min} is the minimum angle between the most energetic jet and the others, E_{min} (E_{max}) are the minimum (maximum) jet energy from the 4 jet topology of the event,
- the minimum invariant jet mass had to be greater than 500 MeV when forcing the event into 4 jets,
- the $\log(\mathrm{y}_{43})$ had to be greater than -7,
- the $\log(\mathrm{y}_{54})$ had to be greater than -8.

After this preselection, the main background events were the four-fermion events and the $\mathrm{f\bar{f}}\gamma$ QCD events with hard gluon radiation. We observed 4180 events in the data for 4096 expected events from background processes. The preselection efficiencies were varying from 62% to 96% for the 6-jet signals, and from 68% to 98% for the 10-jet signals, depending on the simulated masses.

The 6- and 10-jet analyses were based on a neural network method for the optimization of the background and signal discrimination. The neural network package used was MLPFit. The discriminating variables were used as inputs of the one hidden layer neural

network. The signal output node was used for the signal selection. Each neural network (one per mass window, see further) was trained on 200 GeV simulated background and signal samples. The training was done on the whole range of simulated signal masses belonging to the window analysis.

Jet algorithm variables

As it will be described below, jet algorithm variables (-log(y_{nm})) were used as inputs for the neural networks. One example of these variables (normalized between 0 and 1) at 192-202 GeV is shown in Figure 4-b. On this distribution, an excess of data with respect to Monte-Carlo simulation can be clearly seen at large value of y_{nm} (which corresponds to high number of jets, and consequently to the signal region). Comparable effects were observed for the other variables -log(y_{nm}) with m=7 to 9.

This effect was carefully studied on several data sets, and it was found that the same discrepancy was observed at the Z peak. This disagreement was supposed to come mainly from the modelisation of fragmentation and hadronization processes in high multiplicities of jets. Thus, to achieve this analysis, a correction on these variables had to be applied, in order to better reproduce the data distribution.

The chosen method was the following: the values of each badly described variables from the simulation (namely, -log(y_{nm}) with n=7 to 9) were transformed using a polynomial function, whose parameters were determined requiring that the resulted distribution fit the data distribution. However, determining this function at the Z peak and applying it at 192-202 GeV was not sufficient, since then the effect coming from the 4 fermion events were not taken into account. Thus, as the 189 GeV analysis showed no presence of signal [22], it was decided to use these data and simulation samples to find the correction.

As expected, the same kind of discrepancy was observed at 189 GeV (Figure 4-a). Using integration of these distributions, polynomial functions of the 4th order were obtained, and applied on simulation (see Figure 4-c for the corresponding corrected variable at 189 GeV). Then, these polynomial functions were used at 192-202 GeV to correct the simulation (Figure 4-d). In what follows, the corrected distributions were used and the results obtained are preliminary since these corrections of the Monte-Carlo are under study.

Direct decay of $\widetilde{\chi}_1^0\widetilde{\chi}_1^0$ or $\widetilde{\chi}_1^+\widetilde{\chi}_1^-$ into 6 jets

Events with low chargino or neutralino masses have a large boost and look like 2-jet events. On the contrary, heavy chargino or neutralino events are almost spherical with 6 well separated jets. Therefore, we distinguished 3 mass windows to increase the sensitivity of each signal configuration:

- window N1; low masses: $10 \leq m_{\tilde{\chi}} \leq 42.5$ GeV/c^2,
- window N2; medium masses: $42.5 < m_{\tilde{\chi}} \leq 72.5$ GeV/c^2,
- window N3; high masses: $m_{\tilde{\chi}} > 72.5$ GeV/c^2.

A mass reconstruction was performed using a method depending on the mass window. For the N1 window analysis, the events were forced into 2 jets and the average of the masses was computed. For the two last windows, the events were forced into 6 jets and criteria on di-jet angles were applied to choose the best 3-jet combination.

Three neural networks were used (one per mass window), with the 12 following variables as inputs:

- thrust,
- dist$_{WW}$= $\sqrt{\frac{(M_1-M_2)^2}{\sigma_-^2}+\frac{(M_1+M_2-2M_W)^2}{\sigma_+^2}}$ with M_1 and M_2 were the di-jet masses of the jet combination which minimized this variable (after forcing the event into 4 jets); we took $M_W = 80.4$ GeV/c^2 for the W mass, $\sigma_- = 9.5$ GeV/c^2 and $\sigma_+ = 4.8$ GeV/c^2 for the mass resolutions on the difference and the sum of the reconstructed di-jet masses respectively; this variable is peaked to 0 for WW events, allowing a good discrimination against this background,
- energy of the least energetic jet $\times$ minimum di-jet angle in 4 and 5 jet configurations,
- energy difference between the 2 objects after the mass reconstruction,
- reconstructed mass,
- -log(y$_{nm}$) with n=4 to 9 (for n=7 to 9, the corrected variables were used).

Figure 5 shows the number of expected events from the Standard Model and the number of observed events as a function of the average signal efficiency for the N3 mass window. No excess of events was seen in the data with respect to the Standard Model expectations, therefore we optimized the cut on the neural network by minimizing the expected limit on the excluded cross-section. Mass reconstruction are shown in Figure 6 for two $\widetilde{\chi}_1^0$ $\widetilde{\chi}_1^0$ signals after the neural network selection. In order to obtain signal efficiencies, the full detector simulation was performed on neutralino pair production with a 5 GeV/c^2 step grid in the neutralino mass (20 to 98 GeV/c^2). The efficiencies were typically around 20-40% at the values of the optimized neural network outputs, depending on the simulated masses. The statistical errors on the efficiency was typically 1.5%. The expected and observed numbers of events are reported in Table 7 for each mass window. No excess was observed for any working point.

Indirect decay of $\widetilde{\chi}_1^+$ $\widetilde{\chi}_1^-$ into 10 jets

The indirect decay of charginos gives events with 6 to 10 jets, depending on the decay of the two off-shell W bosons. To take into account the effect of the mass difference ΔM between chargino and neutralino on the topology of the event, we divided the 10-jet analysis into 2 windows:

- window C1; low chargino neutralino mass difference: $\Delta M \leq 10$ GeV/c^2,
- window C2; high chargino neutralino mass difference: $\Delta M > 10$ GeV/c^2.

Two neural networks were trained with 10 discriminating variables as input nodes:

- thrust,
- dist$_{WW}$ as described above,
- energy of the least energetic jet $\times$ minimum di-jet angle in 4 and 5 jet configurations,
- -log(y$_{nm}$) with n=4 to 9 (for n=7 to 9, the corrected variables were used).

The expected number of events from the Standard Model and the number of selected data events as a function of the average signal efficiency are shown for the C2 window (Figure 7). The optimal neural network outputs have been derived with the same procedure as for the 6-jet analysis. No significant excess was found in the number of observed events. The signal efficiencies were obtained by simulating chargino pair production by step of 10 GeV/c^2 on the masses in a 2-dimensional grid (from 20 to 90 GeV/c^2 for $\widetilde{\chi}_1^0$ and from 50 GeV/c^2 to 98 GeV/c^2 for $\widetilde{\chi}_1^+$). These efficiencies were between 10% and 60%,

and the statistical errors around 1.5%. Table 8 summarizes the comparison between data and background expectations.

3.2.2 $\bar{\mathrm{U}}\bar{\mathrm{D}}\bar{\mathrm{D}}$ term: smuons and selectrons searches

Searches for selectrons and smuons were performed in the case of indirect decays (the only possible decay with a $\bar{\mathrm{U}}\bar{\mathrm{D}}\bar{\mathrm{D}}$ term). Due to the existing limit on the chargino mass these analyses were based on the indirect decay of the slepton i.e. the lepton-neutralino channel.

Slepton signals were simulated with SUSYGEN [15] at different slepton masses by a step of 10 GeV/c^2. The points were simulated from 45 to 95 GeV/c^2 for sleptons mass and from 25 to 90 GeV/c^2 for the $\widetilde{\chi}_1^0$ mass up to $\Delta\mathrm{M} = \mathrm{m}_{\tilde{\ell}} - \mathrm{m}_{\widetilde{\chi}^0} = 5$ GeV/c^2.

These two channels have final states with a large hadronic activity and this is true independently on the mass difference between the slepton and the neutralino. The momentum of the lepton coming from the indirect decay of the slepton have been used for the signal selection. Therefore electron and muon identifications were used in these 2-leptons and multi-jets analyses.

Two analysis windows, $\Delta\mathrm{M} \leq 10$ GeV/c^2 and $\Delta\mathrm{M} > 10$ GeV/c^2, with different signal selection optimisation (two different neural networks) have been used, to take into account the mass difference between the slepton and the neutralino. A logical .OR. analysis on the two window mass selections has been used to obtained the final numbers of data and expected background events from SM processes.

Hadronic preselection and lepton identification
First we applied the following hadronic preselection:

- the charged particle multiplicity had to be greater than 15,
- the total energy was required to be greater than $0.6 \times \sqrt{s}$,
- the energy of charged particles was required to be greater than $0.3 \times \sqrt{s}$,
- the effective centre-of-mass energy had to be greater than 150 GeV,
- the $\log(\mathrm{y}_{43})$ had to be greater than -7,
- the $\log(\mathrm{y}_{54})$ had to be greater than -8,
- the thrust had to be lower than 0.94.

The standard electrons and muons identification package of the delphi detector [7] have been used to tag (very loose for electrons and loose for muons, see section 3.1) the two most energetic isolated leptons with opposit charge:

- the momentum of the less energetic tagged lepton has to be greater than 2 GeV/c,
- the energy in a cone of 5 degree around the tagged lepton had to be less than 5 GeV.

After this low level of preselection the remaining number of events for all energies are 2837 for the data and 2688 for the expected background from SM processes.

2e + 6 jets channel: $\bar{\mathrm{U}}\bar{\mathrm{D}}\bar{\mathrm{D}}$ term:selectron

Additional criteria have been applied on the two leptons for the selectron analysis:

- the invariant mass of the two leptons had to be lower than 80 GeV/c^2.
- the theta angle of each lepton had to be between 12 and 168 degrees.

The final signal selection has been done with a neural network trained in the standard back propagation manner [25] with one hidden layer. The following variables have been

used as inputs in the neural network (see Figure 8 and 9):

- the clustering variables y_{43}, y_{54}, y_{65}, y_{76} and y_{87}
- the minimum di-jet mass in the 4, 5 and 6 jet configuration
- energy of the least energetic jet $\times$ minimum di-jet angle in 4 and 5 jet configurations,
- the momentum of the most energetic tagged lepton
- the momentum of the less energetic tagged lepton
- the minimum angle between the tagged and lepton and the nearest charged particle with a momentum greater than 3 GeV/c.

Three output nodes have been defined: one for the signal, one for the $q\bar{q}(\gamma)$ background and one for the 4-fermions.

The final selection of candidate events was based on the signal output value of the neural networks (0.94 for ΔM$\leq$ 10 GeV/c^2 and 0.95 for ΔM$>$ 10 GeV/c^2). The two signal outputs values are shown in Figure 10. After an logical .OR. analysis on the two windows, no excess of data over Standard Model expectations was observed for the selectrons analysis. The numbers of events observed and expected from backgrounds are shown in Table 9.

The signal efficiency was evaluated at each of the 33 simulated points and interpolated in the regions between. Efficiencies for the signal were in the range from 5-40%, for small mass differences, and increased up to 80% for ΔM$>$ 10 GeV/c^2 mass window. The statistical errors on signal efficiencies were typically 2%.

2μ + 6 jets channel: $\bar{\mathrm{U}}\bar{\mathrm{D}}\bar{\mathrm{D}}$ term: smuons

A sequential analysis on the whole mass plane, based mostly on the momenta of the two muons and on the y_{nm} distribution, was performed instead of using a neural network optimisation of the signal selection. The better muon identification efficiency compared with the electron one gave sufficent background rejection with a good signal selection efficiency.

The following criteria have been used for the final 2μ + 6 jets signal selection:

- the maximum muon momentum had to be greater than 10 GeV/c
- the minimum muon momentum had to be greater than 2 GeV/c
- the $-Log(y_{43})$ had to be greater than -6.0
- the $-Log(y_{54})$ had to be greater than -6.5
- the $-Log(y_{65})$ had to be greater than -7.0

No excess of data over Standard Model backgrounds was observed for this analysis. The numbers of events observed and expected from backgrounds are shown in Table 9.

3.2.3 $\bar{\mathrm{U}}\bar{\mathrm{D}}\bar{\mathrm{D}}$ term: squark searches

Searches for stop and sbottom were performed in the case of indirect decays through a single dominant $\bar{\mathrm{U}}\bar{\mathrm{D}}\bar{\mathrm{D}}$ term. The eight quarks event topology depends strongly on the difference in mass between the squark and the $\widetilde{\chi}_1^0$.

SUSY signals were simulated at different squark masses in the range 50–90 GeV/c^2 with $\widetilde{\chi}_1^0$ masses between 30–85 GeV/c^2. The simulated decay used for the efficiency evaluation was $\widetilde{b} \rightarrow b\ \widetilde{\chi}_1^0$ with $\widetilde{\chi}_1^0$ going to three light quarks.

A general hadronic preselection was made with the aim of a high general efficiency for the signal and at the same time a good rejection of low multiplicity hadronic background

events. The selection of the events was optimized for the analysis and applied according to the following criteria:

- the charged particle multiplicity had to be greater than 23,
- the total energy was required to be greater than $0.5 \times \sqrt{s}$,
- the effective centre-of-mass energy had to be greater than 150 GeV,
- the total electromagnetic energy from photons and electrons was required to be less than $0.44 \times \sqrt{s}$,
- the energy of the most energetic photon had to be less than 45 GeV,
- the missing momentum of the event had to be less than 75 GeV/c,
- the - $\log(y_{43})$ had to be less than 6.4,
- the discriminating variable d_α (already defined in chargino analysis),
- the 6 constraints kinematic fit (with 2 equal masses constraint) had to converge.

With this hadronic preselection, which is tighter than the one applied to the neutralino analysis, the number of expected events (2557) was in good agreement with the number of observed events in the data (2559).

The final selection of candidate events was based on the output values of three neural networks (SNNS package). The stop and sbottom analyses were each divided into 2 $\Delta M = m_{\tilde{t}} - m_{\tilde{\chi}^0}$ windows ($\Delta M < 10$ GeV/c^2 and $\Delta M > 10$ GeV/c^2) with different neural networks. Both analyses used the same neural network for the small ΔM window. The following quantities were used as input for the neural networks:

- the total number of charged particles,
- the oblateness of the event,
- -$\log(y_{nm})$ with $m = 4$ to 10,
- the $\chi^2_{M_W}$ of the constraint fit for the W mass reconstruction in 4 jets,
- the variables $\alpha_{min} \times E_{min}$ in the 4 and 5 jet topologies,
- the variable $\beta_{min} \times E_{max}/E_{min}$ in the 4 jet topology.

Sbottom decays produce b-quarks in the final state which may be identified with the impact parameter information provided by the micro-vertex detector. The event tagging obtained with the DELPHI package for tagging events containing a b–quark [28], which calculates the probability to have two b-quarks in the final state, was therefore added as input to the neural network for the sbottom analysis.

No excess of data over Standard Model expectations was observed for both stop and sbottom analyses, therefore a working point optimization on the neural network output was performed minimizing the expected excluded cross-section as a function of the average signal efficiency of the mass window. The numbers of events observed and expected from SM processes are shown in Table 10.

The signal efficiency was evaluated at each of the 30 evenly distributed simulated points in the plane of squark and neutralino masses and interpolated in the regions between. Efficiencies for the signal after the final selection were in the range from 10-20%, for small or large mass differences between squark and neutralino, up to around 50% for medium mass differences. The statistical errors on the signal efficiencies were typically below 2%. The number of expected background as a function of the signal efficiency is shown in Figure 11–a. The reconstructed squark masses for the candidate events after the final cut on the neural network output value is shown in Figure 11–b.

3.3 Sneutrino single production searches

3.3.1 Sneutrino searches in the MSSM framework

The indirect decay channels $\tilde{\nu} \rightarrow \tilde{\chi}^0\nu$ and $\tilde{\nu} \rightarrow \tilde{\chi}^{\pm}l^{\mp}$ already searched for in 1997 and 1998 data [29, 30] were looked for in the data collected by DELPHI in 1999; the results are presented in this note and are still preliminary.

If one takes into account all the decays, violating or not R–parity, of the neutralinos and charginos, the possible final states for both processes $\tilde{\nu} \rightarrow \tilde{\chi}^0\nu$ and $\tilde{\nu} \rightarrow \tilde{\chi}^{\pm}l^{\mp}$ are of two kinds, either purely leptonic: two acoplanar leptons and four leptons, or semi-leptonic (multi-lepton multi-jet). Whereas the cross section for the chargino is much higher than for the neutralino, the cross sections for the purely leptonic and for the multi-lepton multi-jet final states are of the same order, so that it is necessary to look for all kinds of topologies.

Electrons and muons are identified at least at the level of 'loose' identification (see section 3.1); in the following, isolated means that there must be no other charged particle in a 5^o half-cone. In order to select these final states, we first apply a preselection:

- at least two charged particles of standard quality;
- total energy of charged particles E_{ch} greater than $0.1 \times \sqrt{s}$,
- total transverse momentum p_T greater than 5 GeV/c;
- transverse energy[2] E_T greater than 4 GeV or at least one charged particle with p_T greater than 1.5 GeV/c;
- if the number of charged particles $n_{ch} < 7$, less than seven neutral clusters;
- total energy from neutral particles in the event E_{neut} less than $0.4 \times \sqrt{s}$;
- energy of the most energetic shower in the STIC[3] E_{STIC} at most $0.2 \times \sqrt{s}$;
- thrust axis not parallel to the beam pipe: $|cos\theta_{th}|$ less than 0.95 (0.9 if $n_{ch} = 2$);
- absolute value of event charge Q_{ev} at most 1 if $n_{ch} < 7$;
- at least one isolated lepton[4] with momentum above 5 GeV/c.

The efficiency of these requirements, designed for the preselection of the signals generated with a dominant λ_{121} coupling, is on average at $\sqrt{s} = 200$ GeV of 72%, 93% and 90% respectively on the two-lepton, four-lepton and semi-leptonic signals. On the signals generated with a dominant λ_{131} coupling, these numbers become 60%, 75% and 74%.

Then we designed three more series of requirements, in order to select the three kinds of topologies that we search for in each coupling hypothesis.

- Two acoplanar leptons final states (same analysis for both λ_{121} and λ_{131}):
  - we required the charged particle multiplicity to be two,
  - at least one well identified[5] lepton,
  - not two muons identified[4],
  - the momentum of the non-leading particle p_2 had to be less than 35 GeV/c,
  - the acoplanarity below 160^o,
  - the acollinearity above 50^o,
  - y_{21} lower than $10^{-0.5}$,

[2] $E_T = \Sigma\sqrt{p_x^2 + p_y^2 + m^2}$

[3] Very forward calorimeter

[4] 'Loose' selection

[5] 'Tight' selection

- visible mass[6] M_{vis} less than $0.25 \times \sqrt{s}$,
- the invariant mass of the two leptons, M_{ll}, lower than $0.3 \times \sqrt{s}$,

- Four leptons final states:
  - we asked for $3 \leq N_{ch} \leq 6$,
  - at least three (λ_{131}: two) well identified leptons (electrons or muons),
  - y_{43} bigger than $10^{-3.5}$.
- Multi-lepton multi-jet final states:
  - there must be at least 7 charged particles and at most 25,
  - there must be at least two well identified leptons (electrons or muons),

  λ_{121} :
  - the p_T of the second lepton $p_T(l_2)$ had to be above 10 GeV/c,
  - y_{43} had to be bigger than 10^{-3},
  - $n_{tot}(j_1)$, the total multiplicity of the leading jet (when the number of jets was forced to 4) could not exceed 4;

  λ_{131} :
  - one of the identified leptons had to be an electron,
  - the missing energy[7] E_{miss} could not be less than $0.25 \times \sqrt{s}$,
  - $M_{ll} \geq 10$ GeV/c^2,
  - y_{43} had to be bigger than 10^{-3},
  - when the number of jets was forced to 4, the number of jets with a maximum total multiplicity of 4 was required to be at least 2.

The average efficiency of these selections is at $\sqrt{s} = 200$ GeV 42%, 46% and 28% (λ_{131}: 34%, 43% and 18%) respectively on two-lepton, four-lepton and multi-lepton multi-jet signals assuming $\tan\beta = 1.5$; the efficiencies are roughly identical if one assumes $\tan\beta = 30$.

The comparison of the number of observed events and the number of expected events after each criteria of these selections is shown in Table 11. Some important variable distributions are also shown in Figure 5. The background composition in each channel is displayed in Table 12. The three channels being totally independent thanks to the charged multiplicity criterion, they can be summed (see last part of Table 12); there is clearly no excess of data with respect to the SM expectations in any of the three channels.

3.3.2 Single sneutrino searches with the single chargino or single neutralino channel

The previous single production study assumed that the values of the SUSY parameters were those given by the minimal MSSM model (e.g. gaugino mass unification at the GUT scale). Therefore, these results were obtained for charginos and neutralinos with branching ratios given in a proportion determined by the MSSM.

In this paragraph we report on a complementary study where the production of charginos and neutralinos and their subsequent **direct** decay through the couplings λ_{121} was studied separately. The analysis was performed only on the data collected at a centre-of-mass energy of 200 GeV with an integrated luminosity of 83.3 pb^{-1}

The assumption that the lifetime of the LSP is negligible was retained and the signal events were generated by using SUSYGEN 2.20/03 [15] for various values of $m_{\tilde{\nu}}$ and for

[6] $M_{vis}^2 = E_{tot}^2 - \vec{p}_{tot}^2$
[7] $E_{miss} = \sqrt{s} - E_{ch} - E_{neut}$

$\tan\beta = 1.5$.

For the signal simulation the fast simulation program SGV [16] was used. A comparison of the efficiencies in different points in the MSSM parameter space to the DELPHI full simulation and reconstruction program gave acceptable differences of the order of $\Delta\epsilon = \pm\ 5\%$ considering topologies with jets. For pure leptonic topologies the agreement was better.

Single chargino production: Signature $4l^{\pm} + (\not{P}_T)(\lambda_{121})$

A dedicated search for signals from the sneutrino $\tilde{\nu}_\mu$ resonance producing a single chargino (which decay directly) has been performed in the channel $\tilde{\nu}_\mu \rightarrow\ \mu^{\pm}\chi^{\pm}$.

The most interesting final signature involves four charged leptons with or without missing energy. This topology is the most promising signature for the search of the $\not{R}_p$ signals if the chargino direct decay in three charged leptons is dominant (chargino LSP).

The analysis has been performed for the final state of four charged leptons with or without missing energy. The selection criteria and their effect on data and on the simulated background from SM processes are shown in Table 13.

The events were selected according to their number of charged particles (N_{ch}),the total energy (E_{tot}), the energy of the charged particles (E_{ch}) and the energy of the neutral particles (E_{neu}). Conditions were imposed on the energy measured by the STIC calorimeter (E_{STIC}), the momentum of the selected charged particles (P_{ch}) and the polar angle θ.

The second step contained a check of the total charge of the event and a criteria applied on the number of identified leptons (muons or electrons) of the final state (N_{lep}). In the third step conditions on the isolation angle of the final charged particles (θ_{ch}^{min}) were imposed.

The number of events selected in the data and expected from the background sources remaining at the end are also included in Table 13.

The efficiency of the single chargino production $\chi_1^{\pm}$ had a mean value of 35 % for $m_{\chi_1^{\pm}} \geq 90$ GeV/c^2 .

Single neutralino production: Signature $2l^{\pm} + (\not{P}_T)\ (\lambda_{121})$

A search for signals of single neutralino production from the sneutrino $\tilde{\nu}_\mu$ resonance producing single neutralino has also been performed in the channel $\tilde{\nu}_\mu \rightarrow \tilde{\chi^0}\nu$.

The analysis has been performed for the final state of two charged leptons with missing energy. The events selected have satisfied the criteria given in Table 14. The preselection criteria imposed conditions on the momentum (P_{ch}), the polar angle θ and the number N_{ch} of the charged and neutral N_{neu} particles. Criteria on the energy of the charged (E_{ch}) and neutral (E_{neu}) particles and the energy of the STIC calorimeter (E_{STIC}) were also imposed. The second step included restrictions on the number of leptons (N_{lep}), their isolation angle (θ_{lep}^{min}) and the missing energy (E_{miss}). Finally the third step imposed criteria on the missing transverse momentum ($\Sigma\not{P}_T$) and the acoplanarity ($Acopl$) of the lepton pair.

The number of data and of background events expected from SM processes are also reported in Table 14. The observed candidate events in the data were in agreement with the SM background. The average efficiency of the signal was 25% for $m_{\chi_1^0} \geq 30$ GeV/c^2.

4 Interpretation of the results in the MSSM framework

The results of the searches presented in this paper were in agreement with the Standard Model expectation. They were used to extend the previously excluded part of the MSSM parameter space and to update limits obtained with similar analyses performed on 1998 data.

4.1 Results from gaugino pair production study with $\mathrm{LL\bar{E}}$ terms

The number of expected events corresponding to gauginos pair production in each point of the explored MSSM parameter space was obtained by:

$$\mathrm{N_{exp}} = \epsilon_g \times \{\sum_{E_{cm}=192}^{E_{cm}=202} \mathcal{L}_{E_{cm}} \times \{\sum_{i,j=1}^{4} \sigma(\mathrm{e^+e^-} \rightarrow \widetilde{\chi}_i^0 \widetilde{\chi}_j^0) + \sum_{k,l=1}^{2} \sigma(\mathrm{e^+e^-} \rightarrow \widetilde{\chi}_k^+ \widetilde{\chi}_l^-)\}\}$$

where $\mathcal{L}_{E_{cm}}$ is the integrated luminosity collected at the centre-of-mass energy E_{cm}, and ϵ_g is the global efficiency determined as explained in section 3.1.1. This number has been compared to the number of signal events, $\mathrm{N_{95}}$, expected at a confidence level (C.L.) of 95% in presence of background, determined following the Bayesian method [31]. All points which satisfied $\mathrm{N_{exp}} > \mathrm{N_{95}}$ were excluded at 95% C.L. The analysis performed considering the λ_{133} coupling as the dominant one provided the most conservative constrains on the MSSM parameter values. The corresponding excluded area in μ, $\mathrm{M_2}$ planes obtained with the present searches are extended as shown in Figure 13, for $\mathrm{m_0}$ = 90, 500 GeV/c^2 and tanβ =1.5, 30.

For each tanβ, the highest value of neutralino mass which can be excluded has been determined in the μ, $\mathrm{M_2}$ plane (–200 GeV/$c^2 \leq \mu \leq$ 200 GeV/c^2, 5 $< \mathrm{M_2} \leq$ 400 GeV/c^2) for several $\mathrm{m_0}$ values from 90 to 500 GeV/c^2; the most conservative mass limit was obtained for high $\mathrm{m_0}$ values. The corresponding limit on neutralino mass as a function of tanβ is shown in Figure 14.
The same procedure has been applied to determine the most conservative lower limit on the chargino mass. The result is less dependent on tanβ, allowing to almost reach the kinematical limit for any value of tanβ.
The lower limit obtained on the neutralino mass is 37 GeV/c^2, and the one on the chargino mass is 99 GeV/c^2.

4.2 Results from gaugino pair production study with $\mathrm{\bar{U}\bar{D}\bar{D}}$ terms

The number of signal events ($\mathrm{N_{95}}$) expected at 95% confidence level with presence of background was calculated from data and SM event numbers obtained for all energies [32]. The signal efficiency for any value of $\widetilde{\chi}_1^0$ and $\widetilde{\chi}^{\pm}$ masses was interpolated using an efficiency grid determined with signal samples produced with the full DELPHI detector simulation. For typical values of tanβ and $\mathrm{m_0}$ (the common scalar mass at the GUT scale), the (μ,M_2) point was excluded at 95% confidence level if the expected number of signal taking into account the selection efficiency at this point was greater than the $\mathrm{N_{95}}$.

Adding the 6-jet analysis (used for the direct decay of $\widetilde{\chi}_1^0\widetilde{\chi}_1^0$ or $\widetilde{\chi}_1^+\widetilde{\chi}_1^-$) and the 10-jet analysis (used for the indirect decay of $\widetilde{\chi}_1^+\widetilde{\chi}_1^-$) results, an exclusion contour in the (μ, $\mathrm{M_2}$) plane at 95% confidence level was derived for different values of $\mathrm{m_0}$ (90 and 300 GeV/c^2)

and tanβ (1.5 and 30). The results obtained for the energies from 192 to 202 GeV were combined to obtain the exclusion contours shown in Figure 15. In the exclusion plots the main contribution comes from the study of the chargino indirect decays with the 10-jet analysis, due to the high cross-section. The 6-jet analysis becomes crucial in the exclusion plot for low tanβ value, low m_0 values and negative μ values. 95 % C.L. lower limits on the mass of the lightest neutralino and chargino are obtained from the scan on tanβ value from 0.5 to 30. The lower limit on the neutralino mass of 35 GeV/c^2 is obtained for tanβ equal to 1 and m_0 = 500 GeV/c^2 (Figure 16). The chargino is mainly excluded up to the kinematic limit at 99 GeV/c^2. Note that these results are valid for a neutralino mass greater than 10 GeV/c^2.

4.3 Results from slepton pair production study with $\mathrm{LL\bar{E}}$ terms

The results of the searches for 4μ, $2e2\mu$ and $2e2\tau$ final states were used to obtain the number of signal events expected at a confidence level of 95% in presence of background taking into account the efficiencies determined when varying the sneutrino mass. It was compared to the number of expected signal events determined with the $\widetilde{\nu}_e$, $\widetilde{\nu}_\mu$, $\widetilde{\nu}_\tau$ pair production cross-sections and the integrated luminosities at the different centre-of-mass energies. From this comparison, limits on sneutrino mass were derived. The results from the 4τ search were used to derive limits on $\widetilde{\nu}_e$ (λ_{133}) and on $\widetilde{\nu}_\mu$ (λ_{233}), those from the $2e2\tau$ to derive limits on $\widetilde{\nu}_\tau$ (λ_{133}).

For the $\tilde{\nu}$ indirect decay in $\nu\widetilde{\chi}_1^0$ with the $\not{R}_p$ decay of the neutralino via λ_{133}, the efficiencies depend on the sneutrino and neutralino masses. The results of the λ_{133} analysis were used to exclude an area in the $m_{\tilde{\chi}^0}$ versus $m_{\tilde{\nu}}$ plane, as shown in Figure 17. This exclusion area is also valid for the other couplings.

The same procedure has been followed for the charged slepton indirect decays, and the area excluded in the $m_{\tilde{\chi}^0}$ versus $m_{\tilde{\ell}_R}$ plane is plotted in Figure 17. The region where $m_{\tilde{\ell}_R}$ - $m_{\tilde{\chi}^0}$ is less than 2–3 GeV/c^2 is not covered by the present analysis, since then the direct decay becomes the dominant mode, leading to two leptons and missing energy signature. Since the selection of indirect decay of a $\widetilde{\tau}_R$ pair into two taus and two neutralinos is less efficient than for the $\widetilde{e_R}$ or $\widetilde{\mu_R}$ pair, the exclusion plot derived from the analysis results of the $\widetilde{\tau}_R$ indirect decay with a dominant λ_{133} is valid for any slepton flavour in the hypothesis of a branching fraction $\tilde{l}_R \to \ell\widetilde{\chi}_1^0$ equal to 1.

4.4 Results from slepton pair production study with $\mathrm{\bar{U}\bar{D}\bar{D}}$ terms

From the study of selectron and smuon pair production in case of a dominant $\bar{U}\bar{D}\bar{D}$ term, exclusion domains have been computed at 95 % of confidence level with the method developped in [33] (Figures 18 and 19). The MSSM values taken for these exclusion plots were tan β = 1.5 and μ = –200 GeV/c^2. The M_2 value was fixed for each neutralino mass. Due to the existing mass limit on the chargino mass we used 100 % of BR for the decay of the slepton into neutralino lepton. The lower limit on the right-handed selectron was 93 GeV/c^2 for $m_{\tilde{e}_R}-m_{\tilde{\chi}^0} > 10$ GeV/c^2 and 86 GeV/c^2 for $m_{\tilde{e}_R}-m_{\tilde{\chi}^0} >$ 5 GeV/c^2. The lower limit obtained for the right-handed smuon was 88 GeV/c^2 for $m_{\tilde{\mu}_R}-m_{\tilde{\chi}^0} > 10$ GeV/c^2 and 82 GeV/c^2 for $m_{\tilde{\mu}_R}-m_{\tilde{\chi}^0} > 5$ GeV/c^2.

4.5 Results from stop pair production study with $\mathrm{LL\bar{E}}$ terms

From the study of the stop indirect decay to charm and neutralino, with the subsequent $\not{R}_p$ decay of the neutralino in leptons, a lower limit on the stop pair production cross-section was derived as a function of the stop and neutralino masses. Using the efficiencies determined for various values of the neutralino mass, and considering the lowest MSSM cross-section for the stop pair production in case of a maximal decoupling to the Z boson (mixing angle = 56°), the exclusion limit was derived in the $m_{\tilde{t}}$, $m_{\tilde{\chi}^0_1}$ plane, as shown in Figure 20. Taking into account our result on the neutralino mass limit of 37 GeV/c^2 the lower bound on stop mass is 82.5 GeV/c^2 at 95% C.L., valid for a mass difference between the stop and the neutralino greater than 5 GeV/c^2.

4.6 Results from stop and sbottom pair production study with $\mathrm{\bar{U}\bar{D}\bar{D}}$ terms

The exclusion procedure used for the gaugino exclusion was applied to the squark analysis. The resulting exclusion contours for stop and sbottom can be seen in Figure 21. A 100% branching ratio of indirect decays in the neutralino channel was assumed. The mixing angle $\Phi_{mix} = 56°$ ($\Phi_{mix} = 67°$) corresponds to a decoupling of the squarks from the Z boson.

By combining the exclusion contours from the squark searches with the constraint on the neutralino mass from the gaugino searches, lower bounds on the squark masses with $\Delta M = m_{\tilde{q}} - m_{\tilde{\chi}^0} > 5$ GeV/c^2 were achieved. The lower mass limit on the stop is 84 GeV/c^2 in the case of no mixing, and 72 GeV/c^2 in the case of maximal Z-decoupling. The lower mass limit on the sbottom is 80 GeV/c^2 in the case of no mixing. The minimum mixing case for the sbottom results in the lower limit of 71 GeV/c^2 for $\Delta M > 20$ GeV/c^2.

4.7 Results from single sneutrino resonance studies

4.7.1 Limits in the MSSM framework

We have used again the `SUSYGEN 2.20/03` program to scan a wide portion of the MSSM parameter space (127,100 points for each $\tan\beta$) and compute all the cross sections of our final states. The parameter ranges were the same as before[8] [30]. The scans were performed for $\sqrt{s} = 200$ GeV and then rescaled for each of the three other energies.

We used the same method as with 189 GeV data [30] to derive the limits on the λ couplings: in each $(M_{\tilde{\nu}}, \Gamma_{\tilde{\nu}})$ bin, for each parameter set entering this bin, we perform the combination of the three channels and then retain the most conservative obtained limit on the cross-section for this bin. This is done separately for each centre-of-mass energy, and the four samples are then simply combined by keeping the best limit in each bin.

One example of the resulting exclusion plots is shown in Figure 22 for the λ_{131}, $\tan\beta = 1.5$ case: for each scanned sneutrino mass and width, an upper limit on λ_{1j1} is given at 95% C.L.

One can also derive an upper limit on λ_{1j1} as a function of $M_{\tilde{\nu}}$ only, assuming a not too small sneutrino width, e.g. $\Gamma_{\tilde{\nu}} \geq 0.2$ GeV; this is shown in the same figure.

[8] We do not consider parameter combinations that have already been excluded by LEP1 precision studies.

At the best point, namely $M_{\tilde{\nu}} \simeq 200$ GeV where the integrated luminosity is highest, the upper limit at 95% C.L. on λ_{121} is 0.002 and 0.003 on λ_{131}. Because the cross-section is proportionnal to λ^2, the limits on λ are only weakly dependent on the efficiency of the analysis, therefore the results obtained for λ_{131} are almost equivalent to those obtained for λ_{121}.

4.7.2 Limits on single chargino and neutralino produced independently

Very preliminary and partial results can be obtained from the second analysis performed to study the single production. Figure 23 shows the 95% C.L. excluded region for λ_{121} coupling. The smallest efficiency and cross-section is used for this calculation for the chargino mass $m_{\chi_1^\pm} \geq 90$ GeV/c^2. We assume a 100% branching ratio for the reaction $e^+e^- \rightarrow \tilde{\nu_\mu} \rightarrow 4l_i^\pm + (\not{P}_T)$. The smallest coupling at the point of the sneutrino resonance is 0.002. The region excluded by low energy measurements is also indicated in the same figure. Figure 23 shows also the 95% C.L. excluded region for the λ_{121} coupling. We assume a 50% branching ratio for each of the two final topologies $\nu_\mu e^+e^-\nu_e$ and $\nu_\mu e^\pm\mu^\pm\nu_e$. The smallest coupling at the sneutrino resonance is 0.010

5 Summary

A great number of searches for supersymmetry with R–parity violation have been performed on the data recorded in 1999 by DELPHI. Current mass limits for pair produced sparticles are summarized in Table 15 for different $\not{R}_p$ couplings and decay modes.

Apart from pair production, searches have also been performed for gauginos in resonant single sneutrino production, resulting in the following preliminary limits: $\lambda_{121} < 0.002$ and $\lambda_{131} < 0.003$ for $m(\tilde{\nu}) \approx \sqrt{s} = 200$ GeV.

Acknowledgements

The financial support of STINT, The Swedish Foundation for International Cooperation in Research and Higher Education, and NFR, The Swedish Natural Science Research Council, is highly appreciated.

The financial support of the program for Basic Research "Archimidis" of ICCS -NTUA, is highly appreciated.

References

[1] P. Fayet, *Phys. Lett.* **B69** (1977) 489;
G. Farrar and P. Fayet, *Phys. Lett.* **B76** (1978) 575.

[2] S. Weinberg, *Phys. Rev.* **D26** (1982) 287.

[3] For reviews, see e.g. H.P. Nilles, *Phys. Rep.***110** (1984) 1; H.E. Haber and G.L. Kane, *Phys. Rep.* **117** (1985) 75.

[4] V. Barger, G.F. Guidice and T. Han, *Phys. Rev.* **D40** (1989) 2987.

[5] R. Barbier et al., *Report of the group on the R–parity violation*, `hep-ph/9810232`.

[6] B.C. Allanach, A. Dedes and H.K. Dreiner, *Phys. Rev.* **D60** (1999) 075014.

[7] P. Abreu et al., *Nucl. Instr. Meth.* **378** (1996) 57.

[8] F.A. Berends, P.H. Daverveldt, R. Kleiss, *Computer Phys. Comm.* **40** (1986) 271,285 and 309.

[9] S. Nova, A. Olshevski, T. Todorov, DELPHI note 90-53(1990).

[10] S. Jadach, W. Placzek, B.F.L. Ward, *Phys. Lett.* **B390** (1997) 298.

[11] S. Jadach, Z. Was, *Computer Phys. Comm.* **79** (1994) 503.

[12] T. Sjostrand, *Computer Phys. Comm.* **82** (1994) 74.

[13] F.A. Berends, R. Kleiss, R. Pittau, *Computer Phys. Comm.* **85** (1995) 437.

[14] J. Fujimoto *et al.*, *Computer Phys. Comm.* **100** (1997) 128.

[15] S. Katsanevas, P. Morawitz, *Computer Phys. Comm.* **112** (1998) 227
.N. Ghodbane hep-ph/9909499.

[16] SGV M. Berggren `http://home.cern.ch/ berggren/sgv.html`

[17] P. Abreu *et al.*, DELPHI Collaboration, Eur. Phys. J. **C13** (2000) 591.

[18] DELPHI Collaboration, CERN EP/2000-059, accepted *Phys. Lett.* **B**.

[19] F. Cossutti, M. Elsing, M. Espirito-Santo, C. Parkes, T. Spassoff, A. Tonazzo, C. Weiser, K. Beloous, V. Hedberg, F. Mazzucato, DELPHI note 99-175 PROG 239.

[20] S. Catani et al., *Phys. Lett.* **B269** (1991) 432.

[21] C. Berat, E Merle, DELPHI 2000-015 CONF 336.

[22] R. Barbier, P. Jonsson and S. Katsanevas, DELPHI 99-96 CONF 283;
R. Barbier, P. Jonsson, S. Katsanevas, N. Vassilopoulos, DELPHI 99-29 CONF 228;
R. Barbier, P. Jonsson and V. Poireau, DELPHI 00-16 CONF 337.

[23] S. Bentvelsen and I. Meyer, Eur. Phys. J. C4 (1998) 623.

[24] Yu.L. Dokshitzer, G.D. Leder, S. Moretti, B.R. Webber, J. High Energy Phys. 08 (1997) 001.

[25] A. Zell et al., SNNS User manual, Version 4.1, Report N 6/95.

[26] MLPfit, written by J.Schwindling, B.Mansoulié and O.Couet. For futher information, see http://home.cern.ch/˜schwind/MLPfit.html.

[27] G. C. Fox, S. Wolfram, *Nucl. Phys.* **B149** (1979) 413..G. C. Fox, S. Wolfram, *Phys. Lett.* **B82** (1979) 134.

[28] P. Abreu et al., Eur. Phys. J., C10 (1999) 415.

[29] F. Ledroit-Guillon and R. López-Fernandéz, DELPHI 98-165 PHYS 805.

[30] N. Benekos, C. Berat, F. Ledroit-Guillon, R. López-Fernandéz, Th. Papadopoulou, DELPHI note 99-79 CONF 266.

[31] R.M. Barnett et al., *Phys. Rev.* **D54** (1996) 1.

[32] Particle Data Group, Phys. Rev. D54 (1996) 1.

[33] A. Read DELPHI 97-158 PHYS 737.

final states	direct decay of	indirect decay of
$6j$	$\widetilde{\chi}_1^0\widetilde{\chi}_1^0$, $\widetilde{\chi}_1^+\widetilde{\chi}_1^-$	
$8j$		$\widetilde{q}\bar{\widetilde{q}}$
$10j$		$\widetilde{\chi}_1^+\widetilde{\chi}_1^-$
$6j + 2l$		$\widetilde{l^+}\widetilde{l^-}$

Table 1: The multi-jet final states covered in this note in the search for neutralino, chargino, squark and slepton pair productions when one $\bar{\mathrm{U}}\bar{\mathrm{D}}\bar{\mathrm{D}}$ term is dominant. The leptonic decays of W^* and Z^* are not listed in these final states since only pure hadronic events have been studied in the chargino analysis.

centre-of-mass energy (GeV)	192	196	200	202
integrated luminosity (pb^{-1})	25.8	76.4	83.3	40.6

Table 2: Data collected by DELPHI in 1999.

Selection criteria for λ_{133}			Data	MC	Signal
	$4 \leq N_{charged} \leq 6$	$N_{charged} \geq 7$	events	S.M.	effi.
Preselection					
+ Acollin	-	$> 7^o$			
+ E_{miss}	$> 30\% \sqrt{s}$	$> 30\% \sqrt{s}$	1220	1187±6	57%
$E_{cone}^{30^o}$	$\leq 53\%$ E_{total}	$\leq 40\%$ E_{total}	667	677±4	52%
N_{lepton} in					
the barrel	≥ 1	≥ 1			
E_{max}^{l}	[2 GeV, 70 GeV]	[5 GeV, 60 GeV]	435	391±3	47%
Isolation	$\Theta_{lepton-track}^{min} \geq 20^o$	$\Theta_{lepton-track}^{max} \geq 6^o$			
	if $N_{charged}$ =4				
	$\Theta_{lepton-track}^{min} \geq 6^o$	$\Theta_{lepton-track}^{max-1} \geq 10^o$			
	if $N_{charged} = 5, 6$	if $N_{lepton} \geq 2$	180	196±3	43%
$N_{neutral} <$	11	15	141	155±2	43%
$N_{electron}$		≥ 1	103	120±2	42%
$\log_{10}(y_{32})$	≥ -2.7	≥ -1.8			
$\log_{10}(y_{43})$	≥ -4	≥ -2.3			
$\log_{10}(y_{54})$		≥ -3	20	21.1±0.7	39%
4 jets					
$E_{min}^{j} \times \theta_{min}^{j1,j2}$	≥ 1 GeV.rad	≥ 5 GeV.rad	16	17.9±0.7	38%
		at least 1 jet with			
	4 charged jets	1 or 2 charged part.			
	if 4j or 5j	4 charged jets if 4j			
		4 or 5 charged j if 5j	14	15.6±0.6	35%

Table 3: LL$\bar{\text{E}}$: Selection criteria used in the search for pair production of neutralinos and charginos with $\not{R}_p$ decay via λ_{133}. nj means n-jet topology, and a charged jet means a jet with at least one charged particle. The number of data and Standard Model background events are reported, as well as the efficiencies obtained for a signal generated for $\tan\beta =$ 1.5, m_0 =90 GeV/c^2, μ =190 GeV/c^2 and M_2 =170 GeV/c^2 (at this point, $\widetilde{\chi}_1^0\widetilde{\chi}_1^0$ is the dominant process).

Selection criteria for slepton pair analysis (λ_{133}, large amount of missing energy)	data	MC	efficiency indirect decay
Preselection stage	1262	1209±5	
$E^{30^o}_{cone} \leq 40\%\ E_{total}$	1138	1101±4	47%
$E_{miss} > 30\%\sqrt{s}$	602	583±3	40%
$N_{charged} \leq 8$ $N_{neutral} \leq 10$	56	52.6±1.3	39%
$2 \leq E^{l}_{max} \leq 70$ GeV at least one isolated lepton 10^o at least 1 lepton in the barrel	33	32.6±0.9	36%
$\log_{10}(y_{32}) \geq -2.7$ $\log_{10}(y_{43}) \geq -4$ case of 4 jets:	8	7.8±0.3	30%
$\theta^{j1,j2}_{min} \geq 20^o$	3	3.9 ±0.3	28%

Table 4: LL$\bar{\text{E}}$: Selection criteria applied to select slepton pair decays via λ_{133} with a large missing energy in the final state. The number of data and Standard Model background events are reported, as well as the efficiencies obtained for a $\widetilde{\nu}_e\bar{\widetilde{\nu}}_e$ signal generated with $m_{\widetilde{\nu}_e} = 80$ GeV/c^2.

Selection criteria for slepton pair analysis (λ_{133}, small amount of missing energy)	data	MC	efficiency direct decay
Preselection stage	1262	1209±5	
$E^{30^o}_{cone} \leq 50\%\ E_{total}$	1133	1103±4	66%
at least one tight electron	611	565±5	65%
$25 \leq E^{l}_{max} \leq 80$ GeV at least one isolated lepton 10^o at least 1 lepton in the barrel	353	331±2	60%
$N_{charged} \leq 7$, $N_{neutral} \leq 10$	15	12.8±0.7	57%
$\log_{10}(y_{32}) \geq -2.7$ case of 4 jets:	7	8.3±0.6	56%
$\theta^{j1,j2}_{min} \geq 20^o$	3	3.2±0.3	50%

Table 5: LL$\bar{\text{E}}$: Selection criteria applied to select 2e2τ final state. The number of data and Standard Model background events are reported, as well as the efficiencies obtained for a $\widetilde{\nu}_\tau\bar{\widetilde{\nu}}_\tau$ signal generated with $m_{\widetilde{\nu}_\tau} = 85$ GeV/c^2.

Selection criteria for stop pair analysis (λ_{133}, indirect decay)	data	MC	efficiency
Preselection stage	1274	1232±5	
acollin. $\leq 80^\circ$ thrust ≤ 0.9	1028	1023±4	55%
E_{miss} >30%$\sqrt{s}$	523	506±3	53%
$N_{charged}$ ≤25 $N_{neutral}$ ≤20	486	474±3	53%
at least 1 lepton in the barrel	368	373±2	50%
5 ≤E^l_{max} ≤ 50 GeV at least one isolated lepton 6^o	220	238±2	46%
at least one tight electron	107	119±2	38%
$\log_{10}(y_{32}) \geq -1.8$ $\log_{10}(y_{43}) \geq -3$ $\log_{10}(y_{54}) \geq -3$ case of 4 jets: min. ch. multiplicity=1, 2	67 26 19	71.9±0.9 27.2±0.6 20.0±0.5	37% 34% 31%

Table 6: LL$\bar{\text{E}}$: Selection criteria used in the search for pair production of stops decaying indirectly.

Window	Data	Backgrounds	ffγ	Four-fermion
N1	27	25.6 $\pm$ 0.6	22.0	3.6
N2	14	13.3 $\pm$ 0.3	3.5	9.8
N3	18	17.6 $\pm$ 0.4	1.9	15.7

Table 7: $\bar{\mathrm{U}}\bar{\mathrm{D}}\bar{\mathrm{D}}$: Number of selected events in data and corresponding expectations from Standard Model processes for the three mass windows of the **6-jet neutralino, chargino** analysis.

Window	Data	Backgrounds	ffγ	Four-fermion
C1	104	106.3 $\pm$ 0.9	19.6	86.7
C2	23	22.0 $\pm$ 0.4	2.6	19.4

Table 8: $\bar{\mathrm{U}}\bar{\mathrm{D}}\bar{\mathrm{D}}$: Number of selected events in data and corresponding expectations from Standard Model processes for the two windows of the **10-jet chargino** analysis.

Analysis	Data	Backgrounds	ffγ	Four-fermion
selectron	21	21.2 $\pm$ 0.6	2.3 $\pm$ 0.3	18.9 $\pm$ 0.5
smuon	6	3.8 $\pm$ 0.2	0.3 $\pm$ 0.09	3.49 $\pm$ 0.16

Table 9: $\bar{\mathrm{U}}\bar{\mathrm{D}}\bar{\mathrm{D}}$: Number of selected events in data and corresponding expectations from Standard Model processes for the two **6-jet +2 leptons** analyses.

Window	Data	Backgrounds	ffγ	Four-fermion
stop and sbottom (no b-tagging) ΔM $<$ 10 GeV	73	73.1$\pm$1.2	11.0	62.1
stop $\Delta M >$ 10 GeV (no b-tagging)	55	50.7$\pm$1.0	6.3	62.1
sbottom $\Delta M >$ 10 GeV (b-tagging)	9	8.3$\pm$0.4	2.5	5.8

Table 10: $\bar{\mathrm{U}}\bar{\mathrm{D}}\bar{\mathrm{D}}$: Number of selected events in data and corresponding expectations from Standard Model processes for the two mass windows of the **8-jet stop and sbottom** analyses.

$2l$-selection:	192 GeV		196 GeV		200 GeV		202 GeV	
criterion #	data	SM MC	data	SM MC	data	SM MC	data	SM MC
Preselection	2279	2128.4	6668	6353.6	6930	6736.9	3312	3168.7
$N_{ch} = 2$	1397	1408.3	4023	4227.5	4177	4460.	2021	2091.5
$N_l \geq 1$	676	586.7	1958	1880.8	1980	1986.8	976	913.
$N_\mu < 2$	610	579.6	1797	1739.3	1771	1838.5	876	852.1
$p_2 > 35$ GeV/c	140	108.7	393	378.3	404	398.7	198	169.8
acop.$< 160^o$	18	9.8	44	40.6	49	44.7	23	16.
acol.$> 50^o$	12	6.4	33	25.8	27	28.6	11	10.
$y_{21} < 10^{-0.5}$	10	5.	23	18.5	21	20.6	10	7.5
$M_{vis} < 0.25\sqrt{s}$	7	3.6	13	12.8	12	15.	5	5.6
$M_{ll} < 0.3\sqrt{s}$	**2**	**2.1**	**4**	**7.1**	**6**	**7.8**	**1**	**3.4**

	$4l$-selection:	192 GeV		196 GeV		200 GeV		202 GeV	
	criterion #	data	SM MC	data	SM MC	data	SM MC	data	SM MC
	Preselection	2279	2128.4	6668	6353.6	6930	6736.9	3312	3168.7
	$3 \leq N_{ch} \leq 6$	628	490.3	1887	1445.3	1949	1542.1	887	718.6
λ_{121}	$N_l \geq 3$	3	1.9	5	5.9	7	5.	5	2.6
	$y_{43} > 10^{-3.5}$	**1**	**0.35**	**0**	**1.**	**0**	**0.7**	**2**	**0.3**
λ_{131}	$N_l \geq 2$	21	13.3	51	45.8	56	51.3	35	21.9
	$y_{43} > 10^{-3.5}$	**4**	**1.1**	**4**	**3.5**	**4**	**2.8**	**4**	**1.**

	Semi-lep.selection:	192 GeV		196 GeV		200 GeV		202 GeV	
	criterion #	data	SM MC	data	SM MC	data	SM MC	data	SM MC
	Preselection	2279	2128.4	6668	6353.6	6930	6736.9	3312	3168.7
	$N_{ch} \geq 7$	228	202.3	679	602.2	712	651.8	365	320.3
	$N_l \geq 2$	19	19.3	65	56.2	58	57.3	25	28.4
λ_{121}	$p_T(l_2) \geq 10$ GeV/c	4	3.1	12	9.4	10	9.5	7	5.2
	$y_{43} > 10^{-3}$	3	2.	8	6.1	9	6.5	4	3.4
	$n_{tot}(j_1) \leq 4$	**0**	**1.**	**4**	**3.1**	**4**	**3.1**	**2**	**1.7**
λ_{131}	$N_e \geq 1$	9	12.1	37	34.8	34	35.	14	17.4
	$E_{\rm miss} > 0.25\sqrt{s}$	8	8.5	25	24.4	23	24.4	11	12.1
	$M_{ll} > 10$ GeV/c^2	7	5.8	17	16.6	17	17.2	9	8.8
	$y_{43} > 10^{-3}$	4	3.7	11	10.6	12	11.	6	5.3
	$n_{jet}(n_{tot} \leq 4) \geq 2$	**1**	**1.**	**4**	**2.9**	**4**	**2.7**	**1**	**1.35**

All mult.:	192 GeV		196 GeV		200 GeV		202 GeV	
	data	SM MC	data	SM MC	data	SM MC	data	SM MC
λ_{121}	3	3.45	8	11.2	10	11.6	5	5.4
λ_{131}	7	4.2	12	13.5	14	13.3	6	5.75

Table 11: **Single sneutrino analysis**: data/Monte Carlo comparison at each step of the event selection.

	$l\nu l\nu$	$\tau\tau(\gamma)$	$\gamma\gamma \to ll$	Bhabha	All
$2l$ at 192	1.9	0.	0.1	0.	2.1
$2l$ at 196	6.5	0.2	0.35	0.	7.1
$2l$ at 200	6.6	0.1	0.55	0.25	7.8
$2l$ at 202	2.95	0.	0.3	0.1	3.4
$2l$ all $\sqrt{s}$	17.95	0.3	1.3	0.35	20.4

	$llll$	$\gamma\gamma \to \tau\tau$	$\mu\mu(\gamma)$	$\mu\mu q\bar{q}$	Bhabha	All
$4l(\lambda_{121})$ at 192	0.35	0.	0.	0.	0.	0.35
$4l(\lambda_{121})$ at 196	0.75	0.15	0.	0.	0.	1.
$4l(\lambda_{121})$ at 200	0.7	0.	0.	0.	0.	0.7
$4l(\lambda_{121})$ at 202	0.3	0.	0.	0.	0.	0.3
$4l$ all $\sqrt{s}$	2.1	0.15	0.	0.	0.	2.35
$4l(\lambda_{131})$ at 192	0.55	0.05	0.	0.	0.35	1.1
$4l(\lambda_{131})$ at 196	1.6	0.15	0.3	0.2	1.	3.5
$4l(\lambda_{131})$ at 200	1.65	0.	0.35	0.2	0.25	2.8
$4l(\lambda_{131})$ at 202	0.65	0.	0.05	0.1	0.1	1.
$4l$ all $\sqrt{s}$	4.45	0.2	0.7	0.5	1.7	8.4

	$llq\bar{q}$	WW-like	$q\bar{q}(\gamma)$	All
leptons+jets(λ_{121}) at 192	0.7	0.25	0.	1.
leptons+jets(λ_{121}) at 196	2.2	0.75	0.05	3.1
leptons+jets(λ_{121}) at 200	2.5	0.55	0.	3.1
leptons+jets(λ_{121}) at 202	1.3	0.4	0.	1.7
leptons+jets all $\sqrt{s}$	6.7	1.95	0.05	8.9
leptons+jets(λ_{131}) at 192	0.1	0.65	0.25	1.
leptons+jets(λ_{131}) at 196	0.3	1.85	0.7	2.9
leptons+jets(λ_{131}) at 200	0.4	2.15	0.15	2.7
leptons+jets(λ_{131}) at 202	0.1	1.05	0.1	1.35
leptons+jets all $\sqrt{s}$	0.9	5.7	1.2	7.95

Table 12: **Single sneutrino analysis**: background composition.

Single chargino production at $E_{cm} = 200$ GeV		
λ_{121} coupling , Signature: $4l^{\pm} + (\not{P}_T)$		
Selection criteria	Observed events	Expected S.M events
$N_{ch} = 4$ $P_{ch} \geq 5$ GeV/c $20^\circ < \theta < 160^\circ$ $E_{STIC} < 15$ GeV $E_{tot} > 40$ GeV $E_{neut} < 20$ GeV $E_{ch} > 30$ GeV	309	290 ± 10
$\Sigma Q_i = 0$ $N_{lep} \geq 2$ at least one μ	13	8.1 ± 0.9
$\theta_{cha}^{min} \geq 10^\circ$	2	1.61 ± 0.14

Table 13: Number of data and SM background events after each selection criteria normalized to the data luminosity of 83.3 pb^{-1} at 200 GeV, for the leptonic topology of single chargino production. In this analysis the direct decay of the chargino in three charged leptons through the coupling λ_{121} is considered.

Single neutralino production at $E_{cm} = 200$ GeV		
λ_{121} coupling , Signature: $2l^{\pm} + \not{P}_T$		
Selection criteria	Observed events	Expected S.M events
$N_{ch} = 2$ $P_{ch} \geq 10$ GeV/c $20^\circ < \theta < 160^\circ$ $E_{STIC} < 10$ GeV $E_{ch} > 40$ GeV $E_{neut} \leq 10$ GeV $\Sigma Q_i = 0, N_{neu} \leq 1$	5798	4902 ± 35
$N_{lep} = 2$ at least one $e^{\pm}$ $\theta_{lep}^{min} \geq 20^\circ$ $E_{miss} > 50$ GeV	11	14.6 ± 1.7
$\Sigma \not{P}_T \geq 30$ GeV/c $Acopl \leq 165^\circ$	8	6.81 ± 1.15

Table 14: Number of data and SM background events after each selection criteria normalized to the data luminosity of 83.9 pb^{-1} at 200 GeV for the leptonic topology of single neutralino production decaying through the coupling λ_{121}.

Pair production of	LL$\bar{\text{E}}$ analyses		$\bar{\text{U}}\bar{\text{D}}\bar{\text{D}}$ analyses	
	direct	indirect	direct	indirect
$\widetilde{\chi}_1^0$	**37**[1]	**37**[1]	**35**[1]	**35**[1]
$\widetilde{\chi}_1^+$	**99**[1]	**99**[1]	**99**[1]	**99**[1]
$\widetilde{e}_R$	**-**	**87**[2]	×	**86**[3]
$\widetilde{\mu}_R$	**-**	**87**[2]	×	**82**[3]
$\widetilde{\tau}_R$	**-**	**87**[2]	×	**-**
$\widetilde{\nu}_e$	**94**	**-**	×	**-**
$\widetilde{\nu}_\mu$	**82**	**82**[4]	×	**-**
$\widetilde{\nu}_\tau$	**82**	**82**[4]	×	**-**
$\widetilde{t}_L$	×	**-**	**-**	**84**[3]
$\widetilde{t}_1$[5]	×	**82**[3]	**-**	**72**[3]
$\widetilde{b}_L$	×	**-**	**-**	**80**[3]
$\widetilde{b}_1$[5]	×	**-**	**-**	**71**[6]

N.B. For the sfermion indirect decay, a 100 % BR into neutralino + fermion is assumed.

× The decay channel is not possible

- The decay channel is not covered

[1] Valid for any m_0 and tanβ and for –200 $< \mu <$ 200 GeV/c^2 and 0 $<M_2 <$ 400 GeV/c^2.
We assumed a neutralino mass greater than 10 GeV/c^2.
LEP1 excluded region have been included in this limit.

[2] Obtained for μ = –200 GeV/c^2 and tanβ = 1.5.
This result is valid for $\Delta M > 3$ GeV/c^2.

[3] Obtained for μ = –200 GeV/c^2 and tanβ = 1.5.
This result is valid for $\Delta M > 5$ GeV/c^2.

[4] Obtained for μ = –200 GeV/c^2 and tanβ = 1.5.
This result is valid for $M_{\widetilde{\chi}^0} > 37$ GeV/c^2.

[5] The limit has been derived considering the mixing angle which gives
the maximal decoupling to the Z boson in the squark pair production.

[6] Obtained for μ = –200 GeV/c^2 and tanβ = 1.5.
This result is valid for $\Delta M > 20$ GeV/c^2.

Table 15: Sparticle mass limits in GeV/c^2 from the DELPHI $\not{R}_p$ pair production searches of supersymmetric particles.

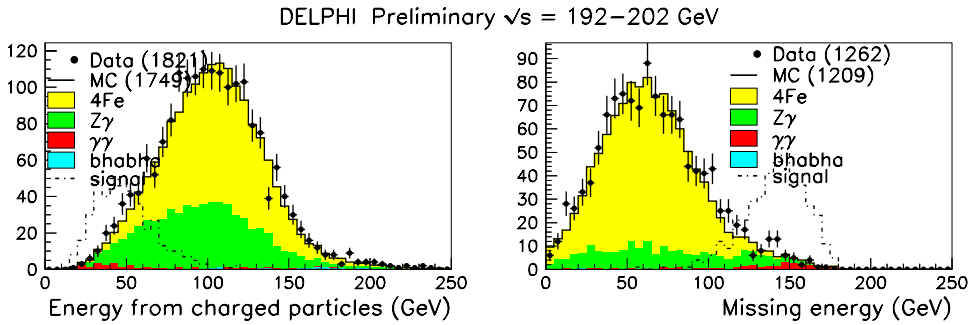

Figure 1: LL$\bar{\text{E}}$: slepton pair search with the λ_{133} coupling: event variable distributions in the preselection. The energy from charged particles (left) and the missing energy (right) distributions are shown.

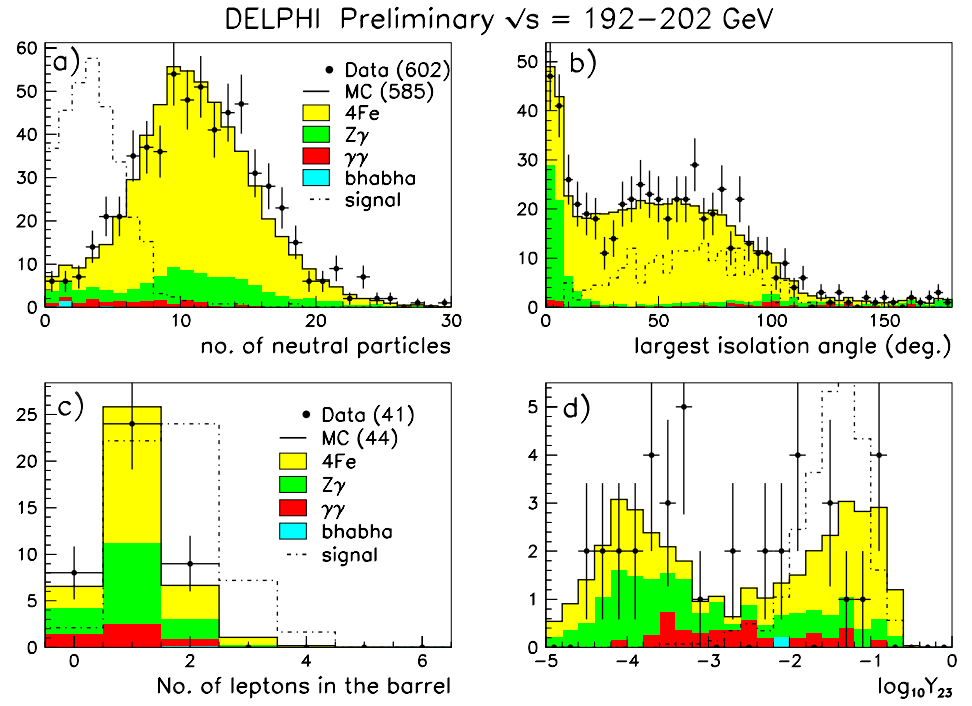

Figure 2: LL$\bar{\text{E}}$: slepton pair search with the λ_{133} coupling: event variable distributions in selection of final state with missing energy.

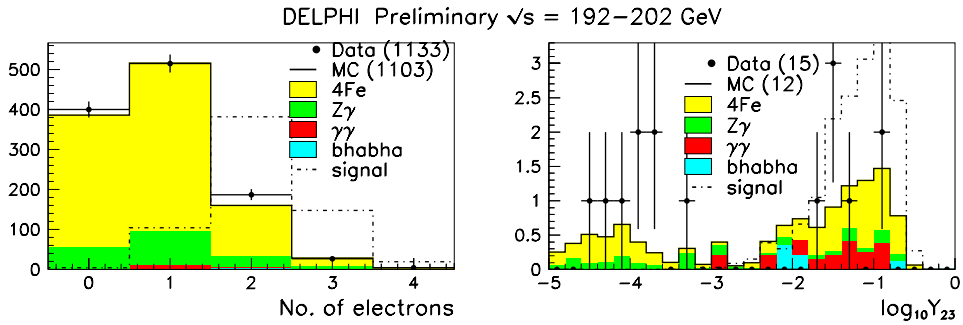

Figure 3: LL$\bar{\text{E}}$: slepton search with the λ_{133} coupling: event variable distributions in selection of final state with small amount of missing energy.

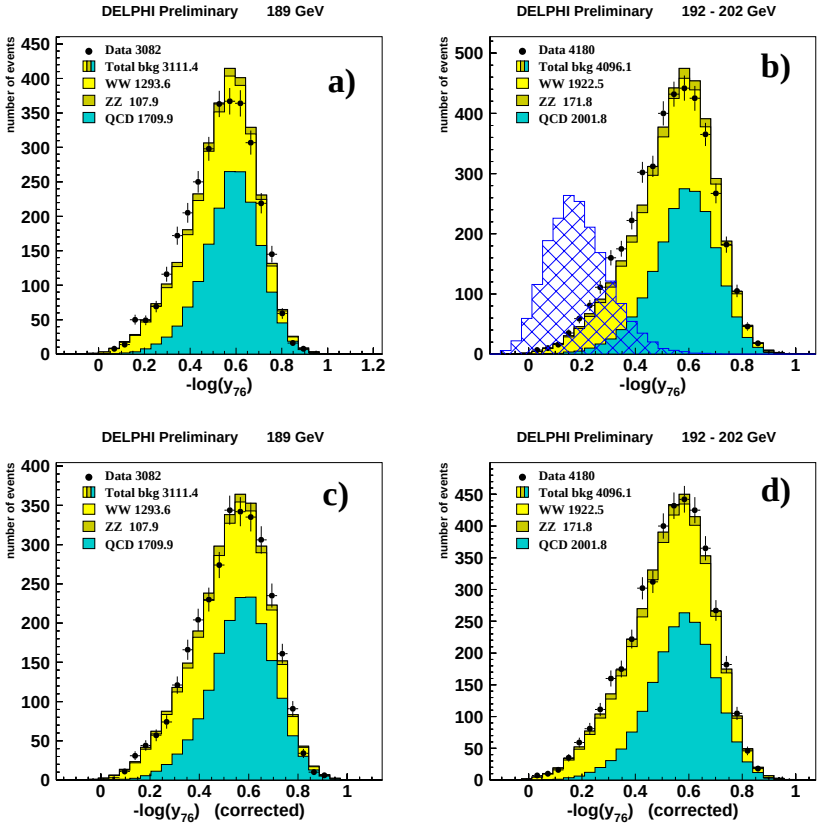

Figure 4: $\bar{\text{U}}\bar{\text{D}}\bar{\text{D}}$ chargino analysis: -log(y_{76}) at 189 GeV before (a) and after (c) the correction, and at 192–200 GeV before (b) and after (d) the correction. The variables were normalized between 0 and 1. The loose hatched histogram is the unweighted signal for the C2 mass window.

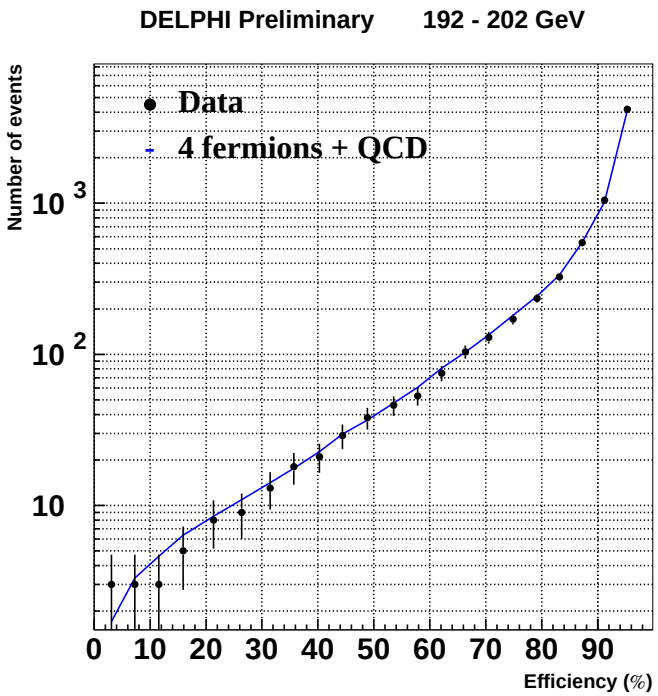

Figure 5: $\bar{\mathrm{U}}\bar{\mathrm{D}}\bar{\mathrm{D}}$: Number of expected events (continuous line) and data events (black dots) versus average signal efficiency for the high neutralino mass search N3.

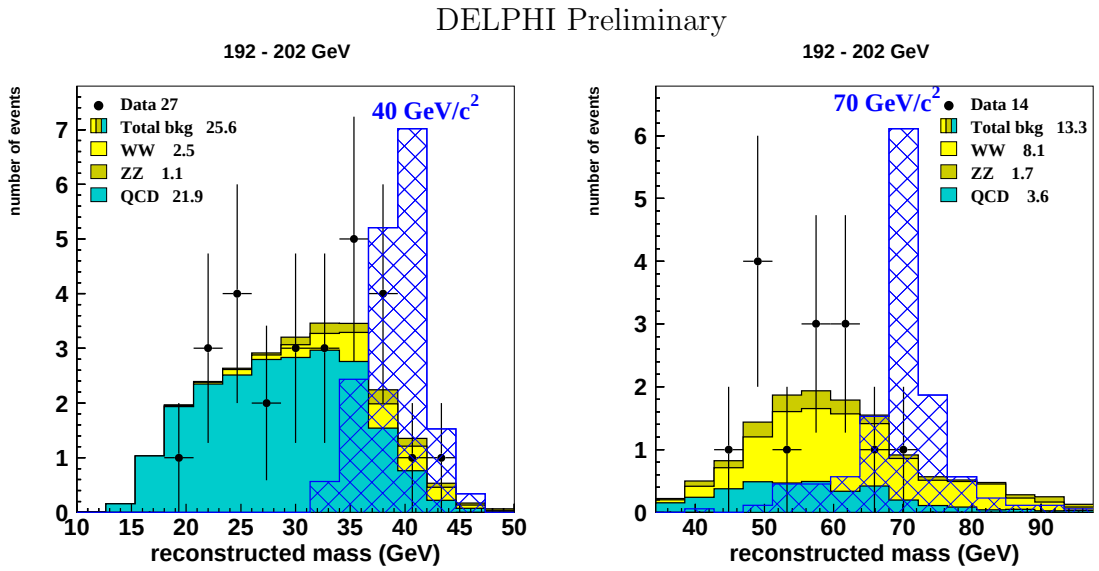

Figure 6: Mass reconstruction for 6-jet events for the background, data (black dots) and for a 40 GeV/c^2 signal (loose hatched histogram) in the N1 window. The right plot shows the reconstruction in the N2 window for a 70 GeV/c^2 signal. The signals are normalized to 1 pb.

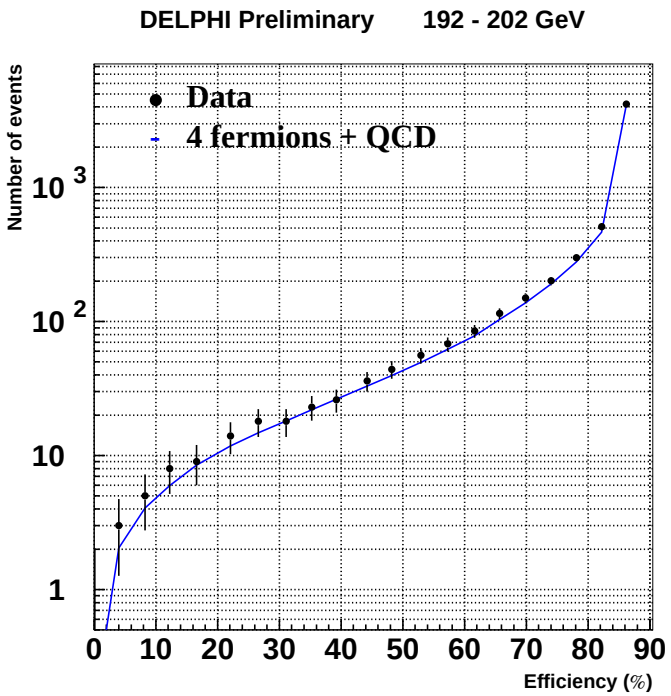

Figure 7: $\bar{\mathrm{U}}\bar{\mathrm{D}}\bar{\mathrm{D}}$: Number of expected events and data events versus average signal efficiency for the analysis applied in case of large ΔM (window C2). The conventions are the same as for the neutralino analysis.

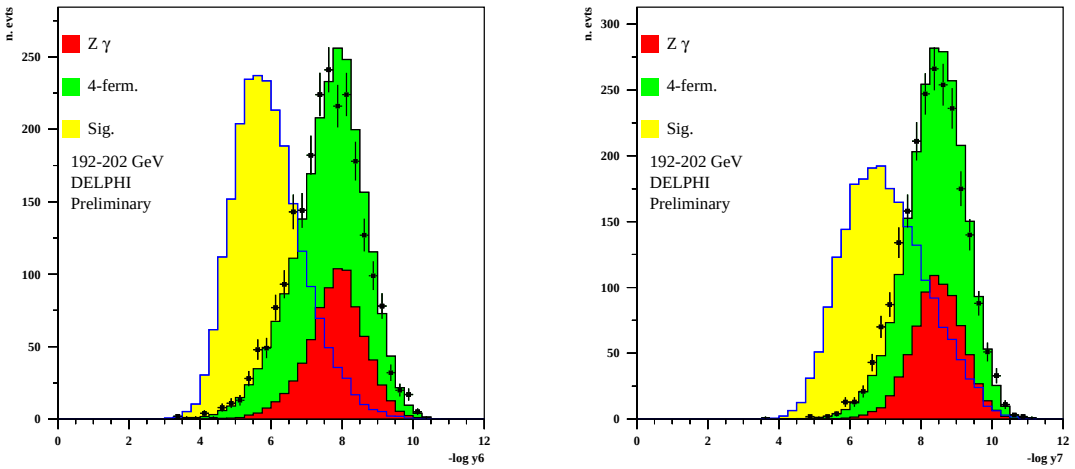

Figure 8: The y_{65} and y_{76} distributions in the $\bar{\mathrm{U}}\bar{\mathrm{D}}\bar{\mathrm{D}}$ selectron analysis.

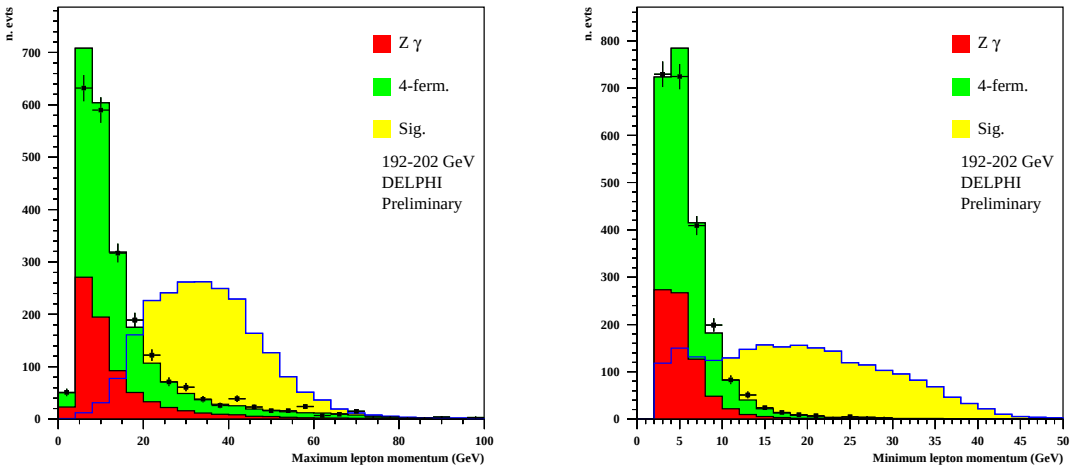

Figure 9: The momentum distribution of the most and the least energetic electrons in the $\bar{U}\bar{D}\bar{D}$ selectron analysis.

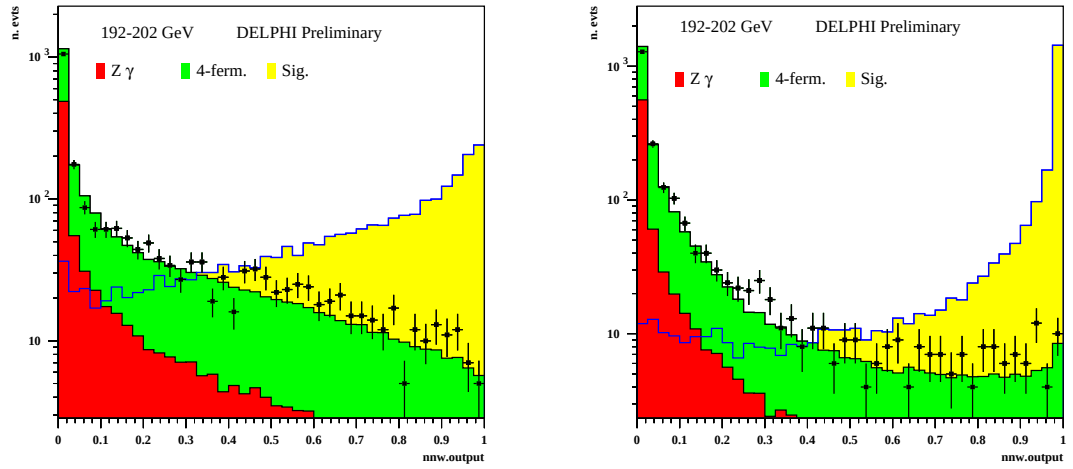

Figure 10: The neural network signal output distribution for the small and large Δ M mass window in the $\bar{U}\bar{D}\bar{D}$ selectron analyses.

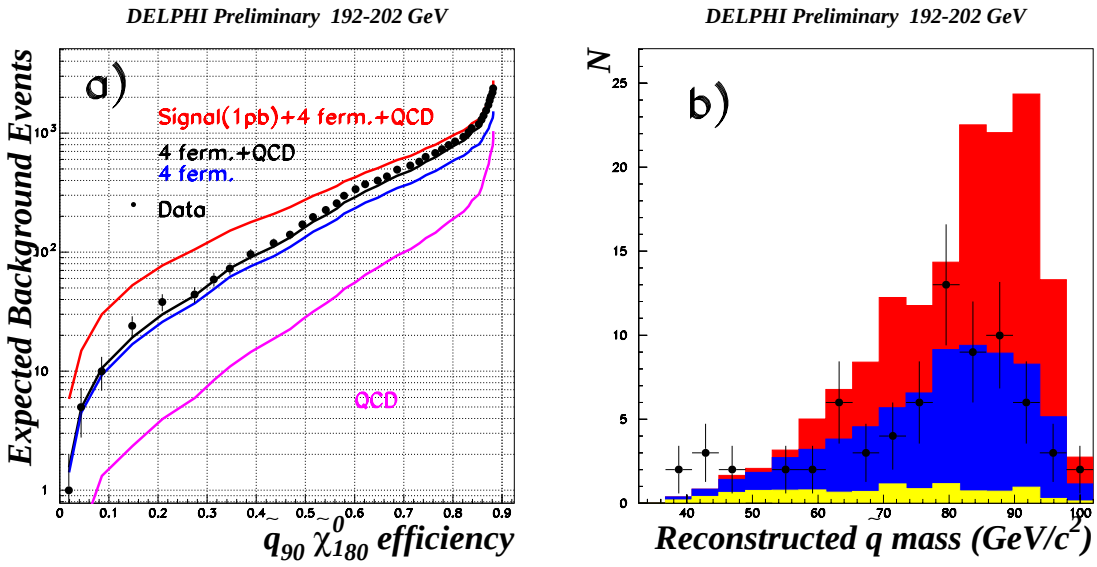

Figure 11: The number of expected background events as a function of the efficiency of an 8-jet signal with a 90 GeV/c^2 squark mass and a 80 GeV/c^2 neutralino mass (a). Reconstructed 8-jet masses (b) after the final event selection for backgrounds (light grey for QCD, dark grey for 4-fermion), an added 90 GeV/c^2 squark signal normalized to 1 pb (medium grey histogram) and data (black dots).

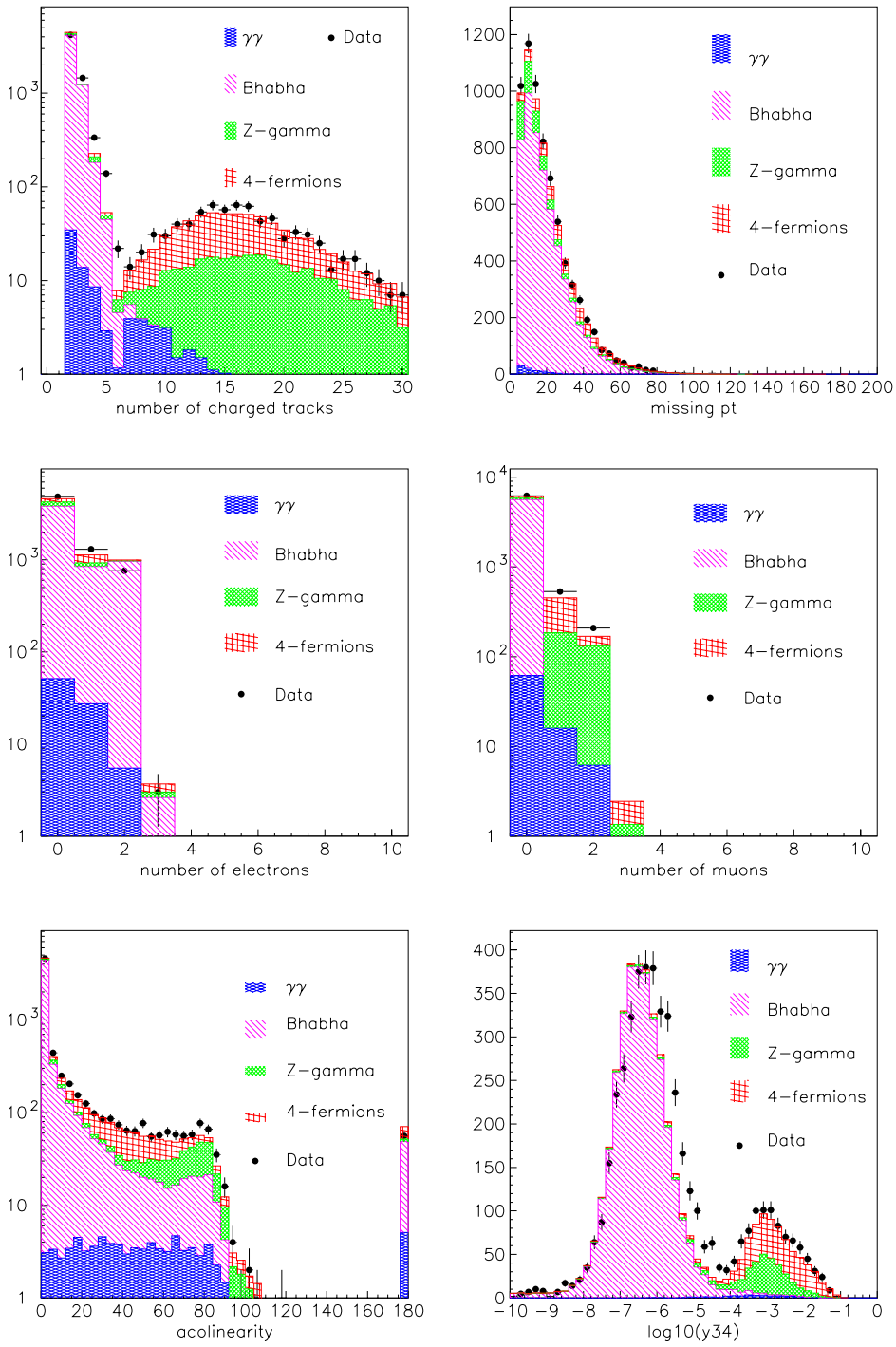

Figure 12: Single sneutrino analysis: data/Monte-Carlo comparison at the preselection level.

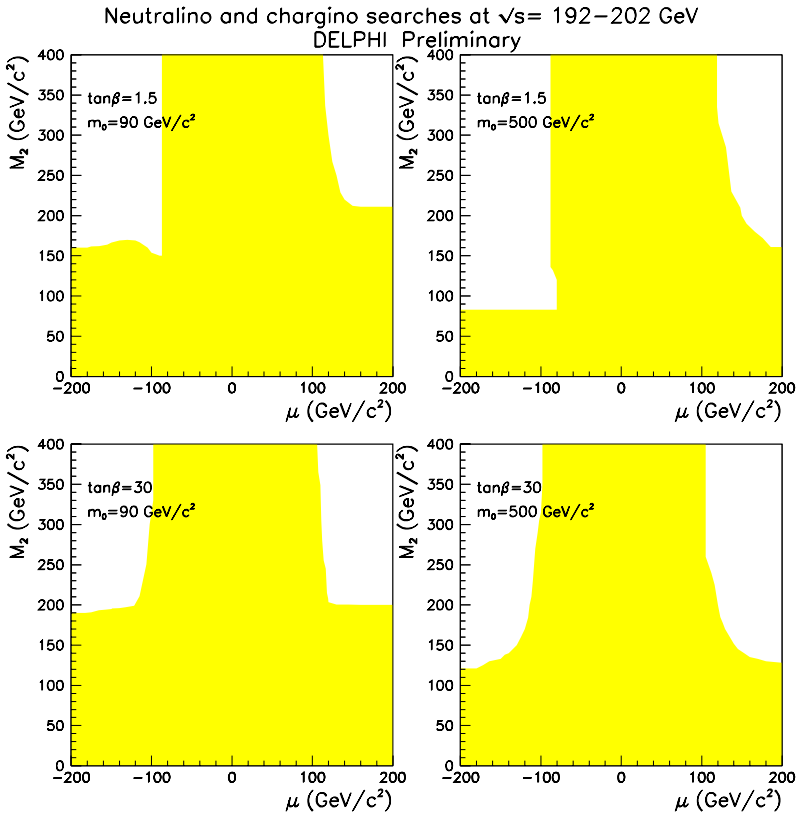

Figure 13: LL$\bar{\text{E}}$: regions in μ, M_2 parameter space excluded at 95 % C.L. by the neutralino and chargino searches for two values of tanβ and two values of m_0.

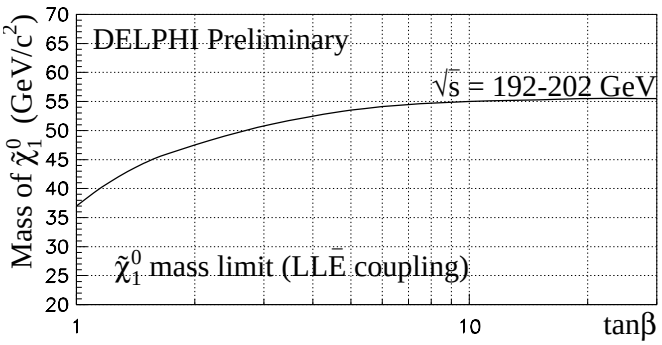

Figure 14: The excluded lightest neutralino mass as a function of tanβ at 95 % confidence level. This limit is valid for all generation indices i,j,k of the λ_{ijk} coupling and all values of m_0.

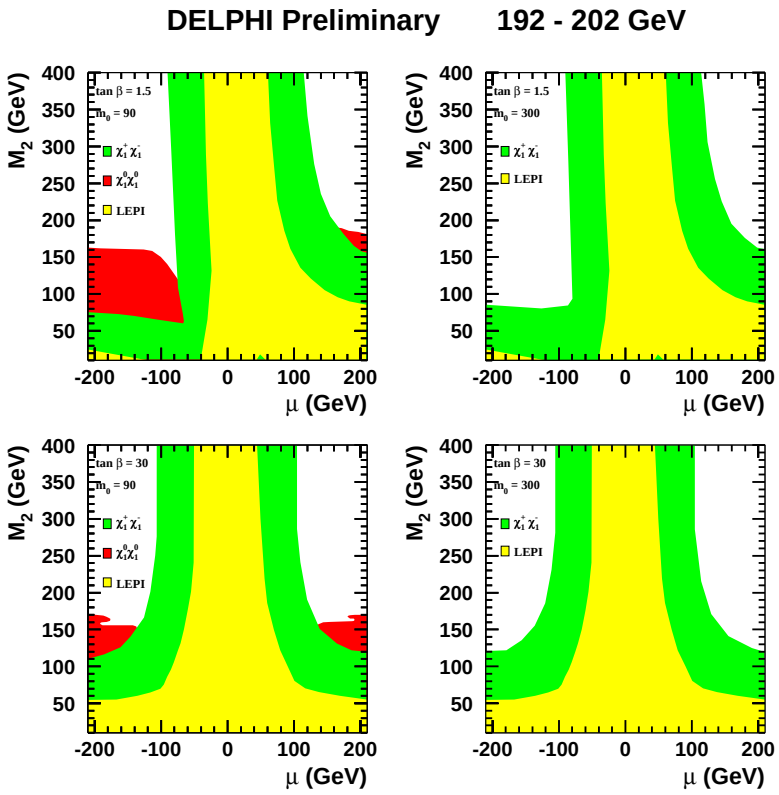

Figure 15: $\bar{\mathrm{U}}\bar{\mathrm{D}}\bar{\mathrm{D}}$ neutralino and chargino searches: exclusion plots in μ, M_2 plane. The 6- and 10-jets analyses are treated separately for this exclusion.

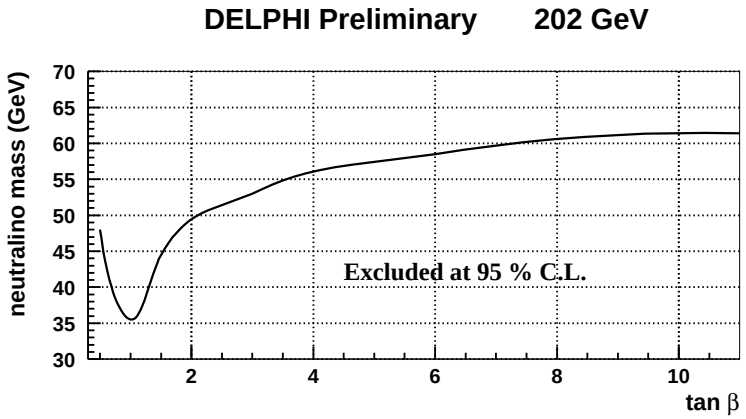

Figure 16: $\bar{\mathrm{U}}\bar{\mathrm{D}}\bar{\mathrm{D}}$: Excluded lightest neutralino mass as a function of tanβ at 95% confidence level.

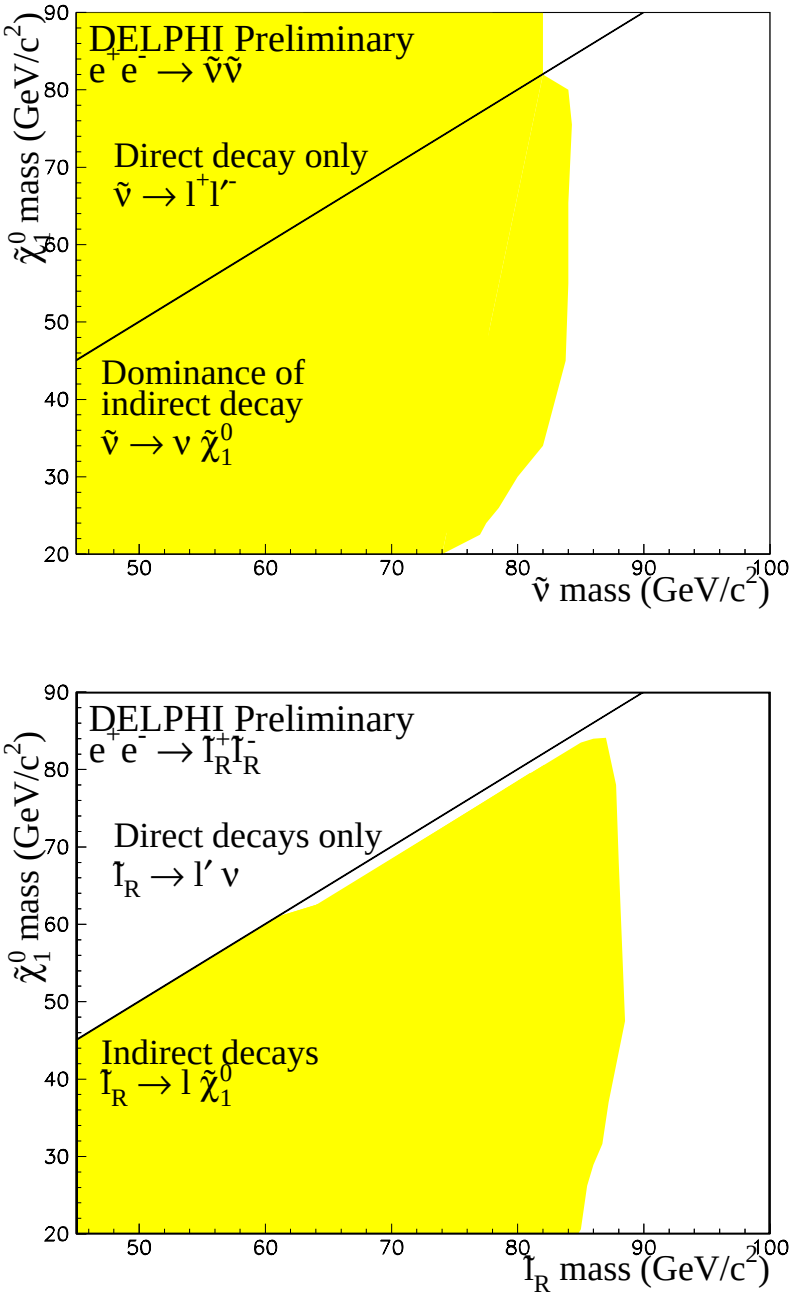

Figure 17: LL$\bar{\text{E}}$: the upper plot shows the excluded region at 95 % C.L. in $m_{\tilde{\nu}}$, $m_{\tilde{\chi}^0}$ plane for $\tilde{\nu}$ pair production for direct and indirect decays. The lower plot shows the excluded region at 95 % C.L. for the charged slepton indirect decay with λ_{133} coupling in $m_{\tilde{\ell}_R}$, $m_{\tilde{\chi}^0}$ plane by $\tilde{\ell}_R$ pair production.

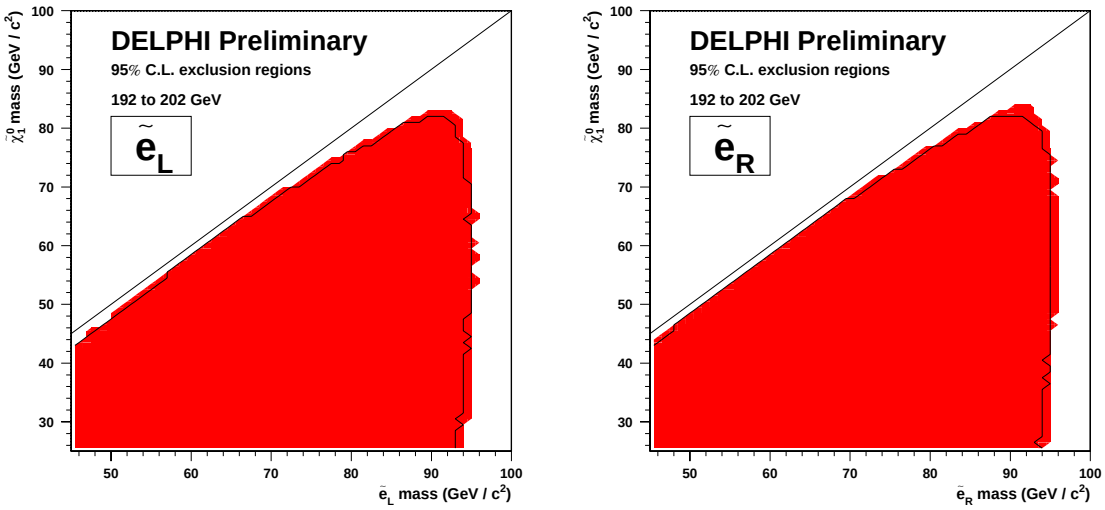

Figure 18: $\bar{\mathrm{U}}\bar{\mathrm{D}}\bar{\mathrm{D}}$: Exclusion domains at 95% confidence level in the $M(\tilde{\chi}_1^0)$, $M(\tilde{e})$ plane for indirect selectron decay in the case of a 100 % branching ratio in the neutralino channel. The superimposed contours illustrate the expected exclusion from the SM background.

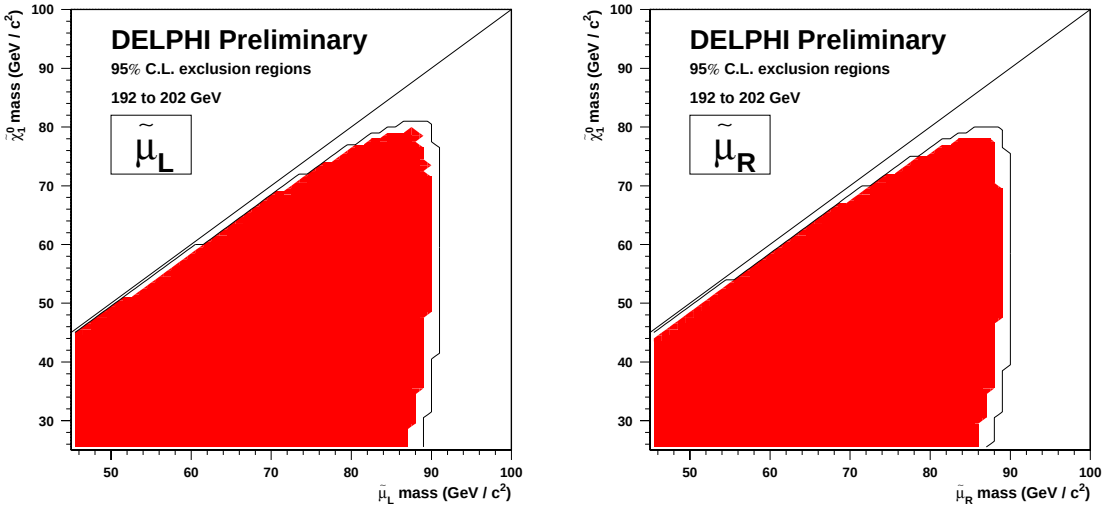

Figure 19: $\bar{\mathrm{U}}\bar{\mathrm{D}}\bar{\mathrm{D}}$: Exclusion domains at 95% confidence level in the $M(\tilde{\chi}_1^0)$, $M(\tilde{\mu})$ plane for indirect smuon decay in the case of a 100 % branching ratio in the neutralino channel. The superimposed contours illustrate the expected exclusion from the SM background.

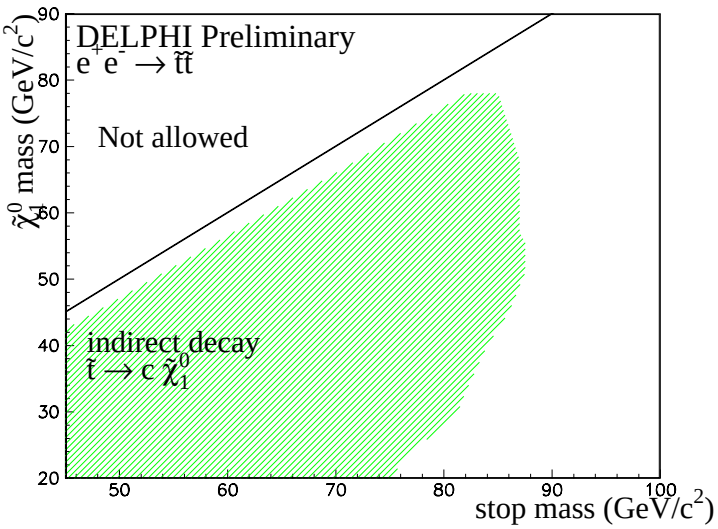

Figure 20: LL$\bar{\text{E}}$: exclusion domain in $m_{\tilde{\chi}^0}$ versus $m_{\tilde{t}}$ for the $\tilde{t}_1$ pair production (with stop indirect decay into $c\tilde{\chi}_1^0$) in case of maximal decoupling to the Z boson.

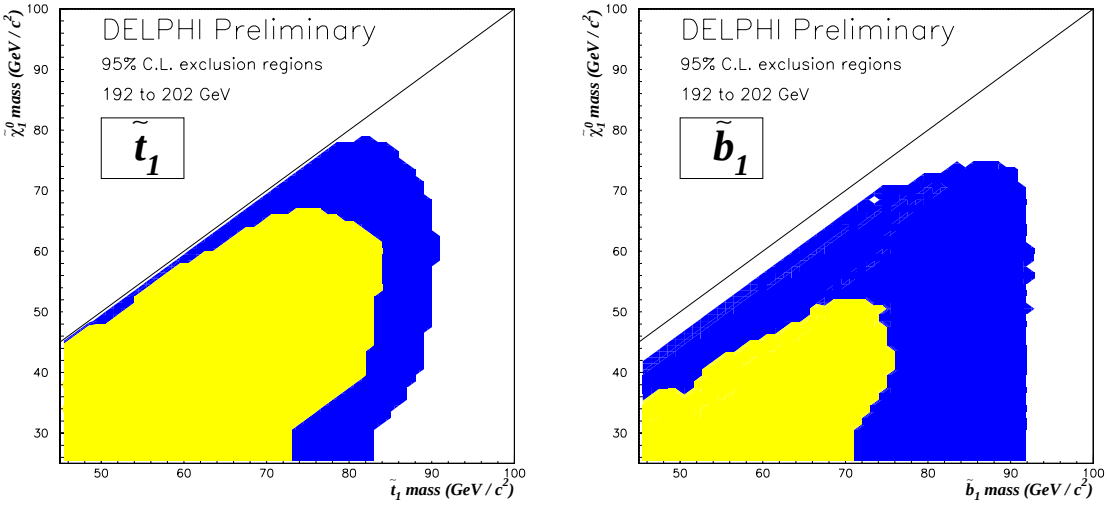

Figure 21: Exclusion contours at 95% confidence level in the $M(\tilde{\chi}_1^0)$, $M(\tilde{q})$ plane for indirect squark decays in the case of a 100 % branching ratio in the quark neutralino channel. The left (right) plot shows the exclusion for a stop (sbottom) in the case of no mixing (dark grey) and with the minimum cross-section producing mixing angle (yellow).

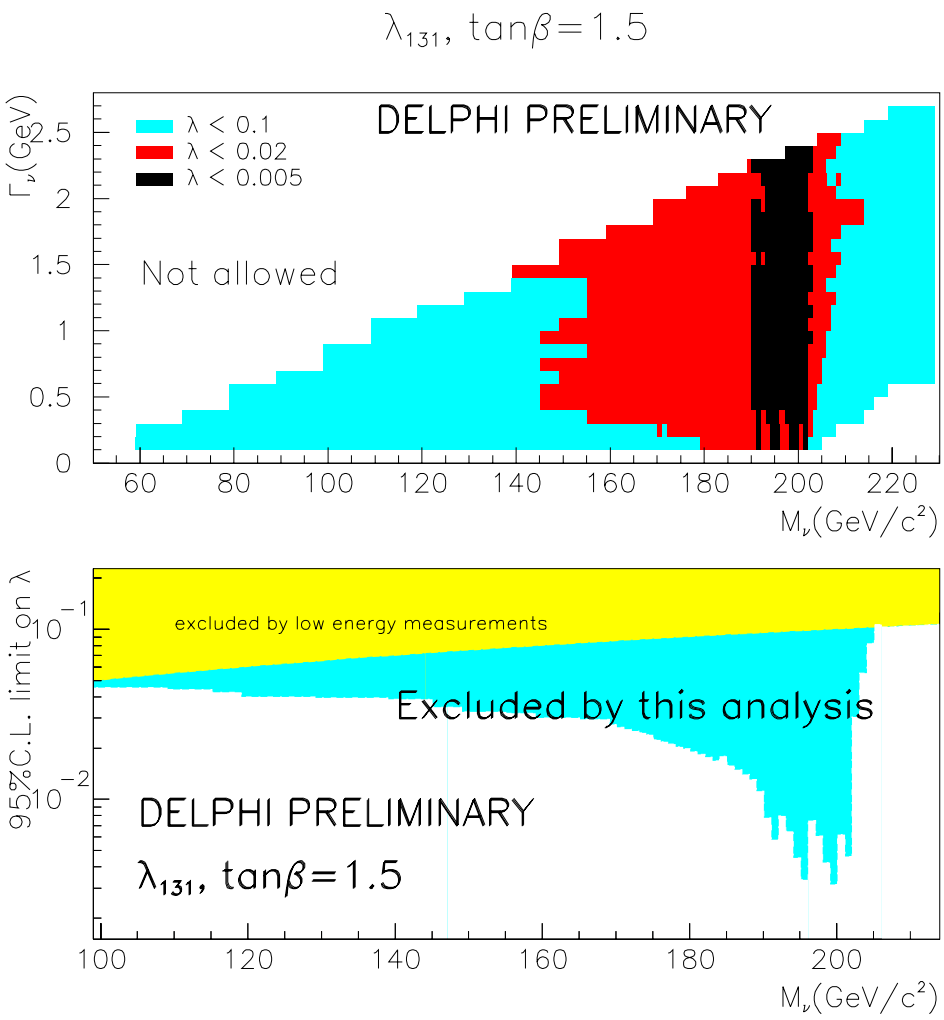

Figure 22: Single sneutrino analysis: for $\tan\beta = 1.5$, upper limit on λ_{131} as a function of $M_{\tilde{\nu}}$ and $\Gamma_{\tilde{\nu}}$ (top) and as a function of $M_{\tilde{\nu}}$, assuming $\Gamma_{\tilde{\nu}} > 0.2$ GeV (bottom). The indirect limit given by low energy measurements is given assuming $M_{\tilde{\nu}} = M_{\tilde{e}_R}$.

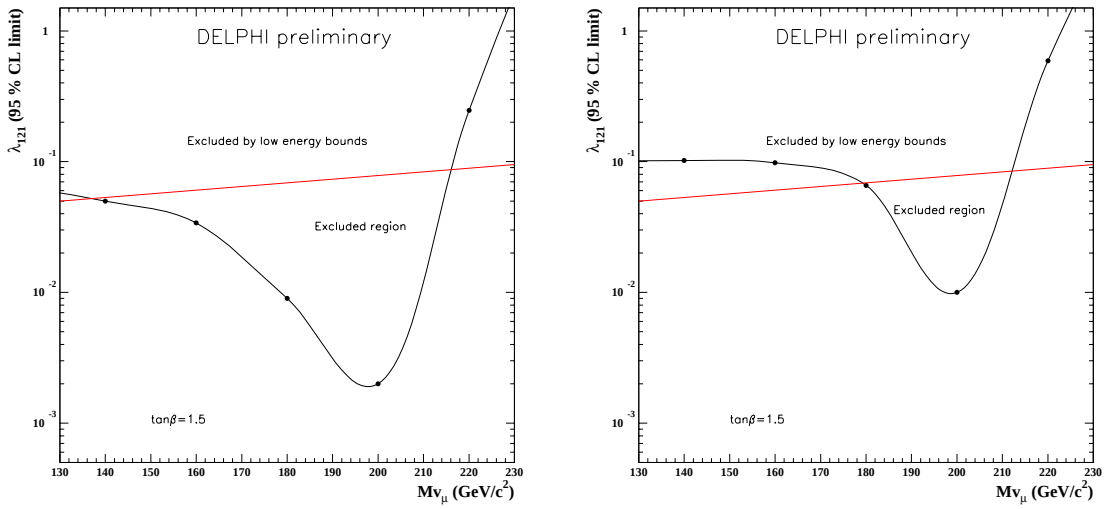

Figure 23: Upper limit for the coupling λ_{121} as a function of $M_{\tilde{\nu}}$ for single chargino production assuming a 100% BR in $4l_i^{\pm} + (\not{P}_T)$ (left) and single neutralino production assuming a 50% BR for $\nu_\mu e^+ e^- \nu_e$ and $\nu_\mu e^\pm \mu^\pm \nu_e$ (right). For both figures, $\tan\beta = 1.5$ is considered. The region excluded by low energy measurements is also indicated.